GEOHISTORY ANALYSIS OF THE MARICOPA SUB-BASIN

Lorelea Samano

ABSTRACT

The Maricopa sub-basin contains sediments and facies sequences recording eustatic, tectonic, and depositional processes that occurred throughout the basin. In order to further understand the timing and effect of tectonic events in the Maricopa sub-basin, three geohistory models were constructed. The models extend across the sub-basin from the southeast to the northwest and were generated using thickness values for the Reef Ridge, Etchegoin, San Joaquin, and Tulare Formations and their litho-stratigraphic equivalents. Isopach maps were constructed from gross thickness values of each of these formations to determine thickness trends of the individual units.

The geohistory models represent basin history from Miocene time to the present (24-0 Ma) and suggest subsidence due primarily to tectonism occurred in the basin as the plate margin transitioned from convergent to transform during Early Miocene time (24-17 Ma). During Middle Miocene time (17-11 Ma), a more stable transform-plate boundary developed to the southeast of the basin causing the region to undergo more subsidence followed by uplift in all regions of the sub-basin. These subsidence and uplift events coincided with wrench tectonics in conjunction with deep-seated thrusting that occurred along the southwest side of the basin (16-17 Ma) (Harding, 1976), as well as an acceleration of the slip rate on the San Andreas fault at 10-12 Ma (Huffman, 1972; Graham 1978; Bartow, 1992). As the more stable transform plate boundary continued to develop to the east of the basin, the geohistory models indicate subsidence occurred in all regions of the sub-basin beginning at ~10 Ma. This subsidence continues to present day in the eastern and central regions of the sub-basin, but ended at ~2 Ma, and was followed by an uplift event in the western region. This uplift event, which persists to present day,

is most likely due to the change in plate motion to a more northerly direction causing compression and uplift parallel to the plate boundary (Page and Engebretson, 1984).

Comparisons of the geohistory models for the Maricopa sub-basin to other models in the San Joaquin basin indicate similarities and differences. The geohistory model for the Tejon embayment suggests that major subsidence and uplift events were controlled by tectonics from the Late Oligocene to the Early Miocene. This is similar to the geohistory analyses for the central and eastern Maricopa sub-basin. However, the Tejon embayment geohistory model shows maximum subsidence occurred earlier (~12 Ma) than it did for the eastern and central Maricopa sub-basin, which show maximum subsidence at present day. Basin development for the Tejon embayment was due to Oligocene/Miocene normal faulting which may not have had as great an influence on basin development of the Maricopa sub-basin (Goodman and Malin, 1992).

Geohistory models created for the Lost Hills area of the San Joaquin basin are somewhat similar in shape to the geohistory models of the Maricopa sub-basin for the later parts of their histories. From ~10 Ma to present, the geohistory models for the 'Bravo' well and those created for the Maricopa sub-basin both exhibit an overall concave downward geometry indicating thrust or sediment loading as the mechanism for subsidence (Bent, 1988). This is typical of a foreland basin setting.

AKNOWLEDGEMENTS

Sincere appreciation is given to my thesis advisor, Jan Gillespie, for the insight she provided on this project and particularly for the help in completing it in a timely manner. I would like to thank my committee members Bob Horton and Stuart Gordon.

I would like to thank my family members for their continuing support throughout all phases of my graduate work. My Mom and Dad and sister Jena supported and encouraged me through the duration of this project as well as my entire life. I also would like to thank the rest of my extended family and friends who were neglected and had to endure the perpetual excuse of "Not right now, I'm working on my thesis," for the last three years.

Thanks are also extended to Geologists Bonnie Bloeser and Don Deininger from Aera Energy LLC, for providing type logs and geologic feedback. Adam Mahan of Aera Energy LLC and Michelle Casterline provided outstanding GeoGraphix and GIS assistance.

Special recognition is given to my friends Stephanie Lewis, John Houghton, and Brian Taylor. Friends who were always there for me when I needed extra support and helped me get through this process.

I would also like to thank The San Joaquin Geological Society and the American Federation of Mineralogical Societies who provided generous Graduate Scholarships for which I am grateful.

TABLE OF CONTENTS

LIST OF FIGURES

INTRODUCTION

The San Joaquin basin is an important petroleum province in California that contains several of the most prolific oil fields in the United States. The basin is bounded on the east by the Sierra Nevada, on the south by the San Emigdio and Tehachapi Ranges, and on the west by the Coast Ranges and San Andreas fault. The Stockton arch (Figure 1) separates the San Joaquin basin from the Sacramento basin to the north. The present study area lies within the Maricopa sub-basin in the southwestern-most region of the San Joaquin basin. The Maricopa sub-basin is separated from the rest of the San Joaquin basin by the Bakersfield arch. The area outlined in Figure 1 represents the boundaries of the study area between T11N, R25W and T11N R20W San Bernardino Base and Meridian to T30S R27E and T30S R23E Mount Diablo Base and Meridian.

The Maricopa sub-basin is a deep structural depression located in the most deformed region of the San Joaquin basin (Bartow, 1991). The sediments deposited within this structural depression record a relatively complete history of Tertiary tectonic events (Bartow, 1991). The complex structural evolution of the basin is a result of the transition from a convergent to a transform plate boundary directly to the west of the basin beginning at ~29Ma (Atwater, 1970). This transition and its effect on the San Joaquin basin is not fully understood (Goodman and Malin, 1992).

In this project, three geohistory models were created for the Maricopa sub-basin to illustrate rates of sediment accumulation through time and also the timing and effects of tectonic events on the sub-basin. The models are compared to other geohistory models for the San Joaquin basin to determine how evolution of the Maricopa sub-basin differed from other areas of the San Joaquin basin.

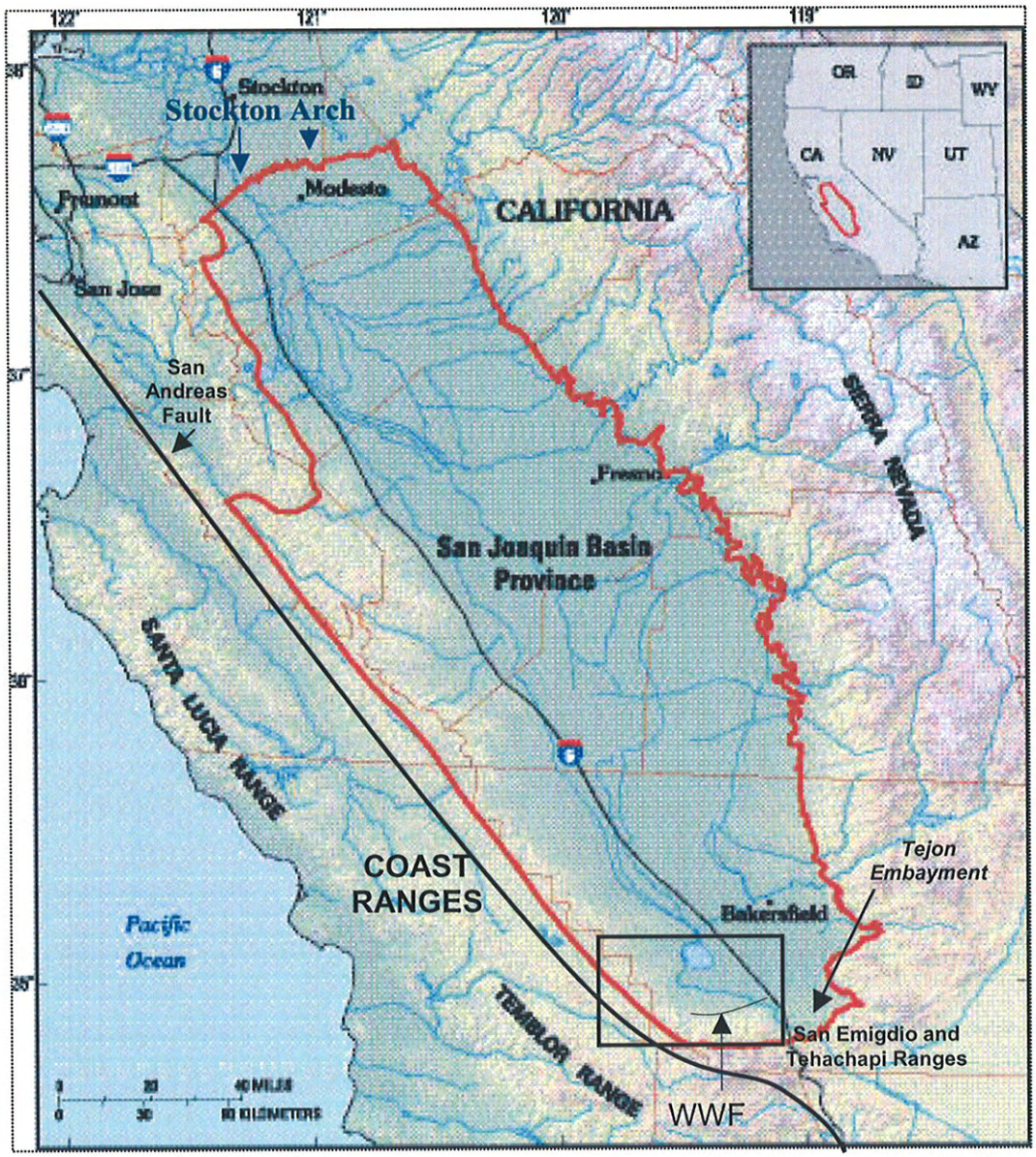

Figure 1. Map showing location of San Joaquin basin province, outlined in red. Within the San Joaquin basin is the Maricopa sub-basin which is contained within the black box. WWF= White Wolf Fault.

Goodman and Malin (1992) performed a geohistory analysis using subsurface data from seismic reflection profiles and well-log data from several hundred wells. Their paper discussed the evolution of the southern San Joaquin basin and related basin development to Middle Tertiary tectonics. The current study evaluates Goodman and Malin's (1992) geohistory model for the easternmost part of the Maricopa sub-basin. Two additional geohistory models for the Maricopa sub-basin were created using the wells highlighted in Figure 2 in order to evaluate how subsidence episodes may have differed throughout the sub-basin.

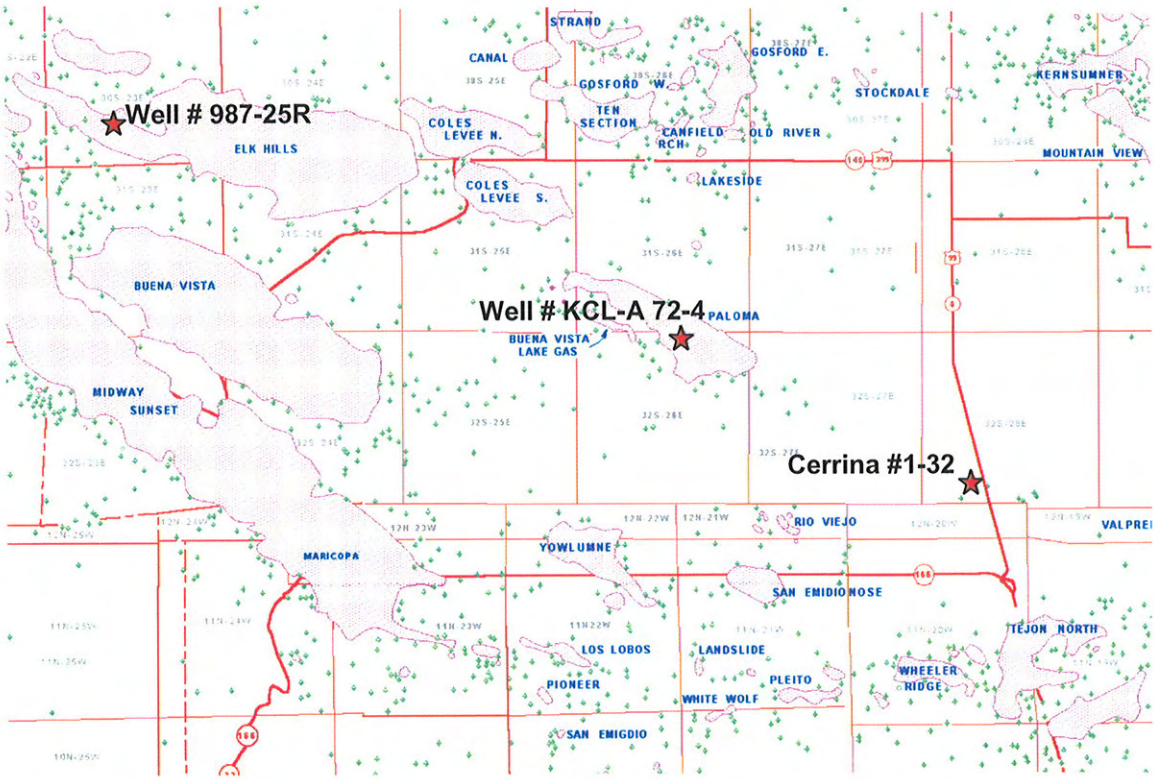

Figure 2. Location of the three wells used for the analyses. The pink shaded areas are the oil fields that fall within the project area. Map from Department of Oil, Gas and Geothermal Resources: ftp://ftp.consrv.ca.gov/pub/oil/maps/Map_S-1.pdf.

PREVIOUS STUDIES

The history of the San Joaquin basin has been of significant interest due to the vast amounts of hydrocarbons located in the valley. Numerous papers and books discussing the tectonic setting, structure, and stratigraphy of the San Joaquin basin have helped to further our understanding of basin evolution through time as well as how it relates to hydrocarbon accumulation.

Tectonics

Atwater (1970) and Atwater and Molnar (1973) proposed a plate-tectonic model that gave a broad synthesis of the tectonic evolution for the western North American plate margin. Their model showed how the plate boundary underwent a transition from a convergent to transform plate setting (Figure 3). Graham (1987) took this plate boundary model further by analyzing sedimentary-basin evolution in the context of transform tectonics superimposed on an older convergent margin and how this related to petroleum occurrences. He concluded that the distribution of oil and gas is clearly controlled by tectonic setting. Nilsen (1987) discussed how California's basins' paleogeography, paleotectonic framework, and depositional history were influenced by tectonics during Paleogene time. He concluded that Paleogene sedimentation in California was strongly affected by sydepositional tectonism, climate changes, and sea-level changes.

Structure

On a more local scale, Davis and Lagoe (1988) wrote about the structural impacts of major tectonic events that affected the western margin of the San Joaquin Valley. They discussed the structural and stratigraphic relationships that document tectonic events and then tied these events to regional relationships that are known through surface mapping by Dibblee (1971, 1973, 1974). These events, which caused deformation along

the western and southern margins of the San Joaquin basin, included the following: development of a westward-vergent thrust belt during the Eocene on the westernmost margin of the valley, development of a fold and thrust belt during Late Eocene to Middle Oligocene along the southern margin of the basin, extensional faulting in the Late Oligocene along the southern margin of the basin, regional basin subsidence from Middle Miocene to Early Pliocene, and fold and thrust belt development along the western and southern margins of the San Joaquin basin during Late Pliocene to Quaternary time (Davis and Lagoe, 1988).

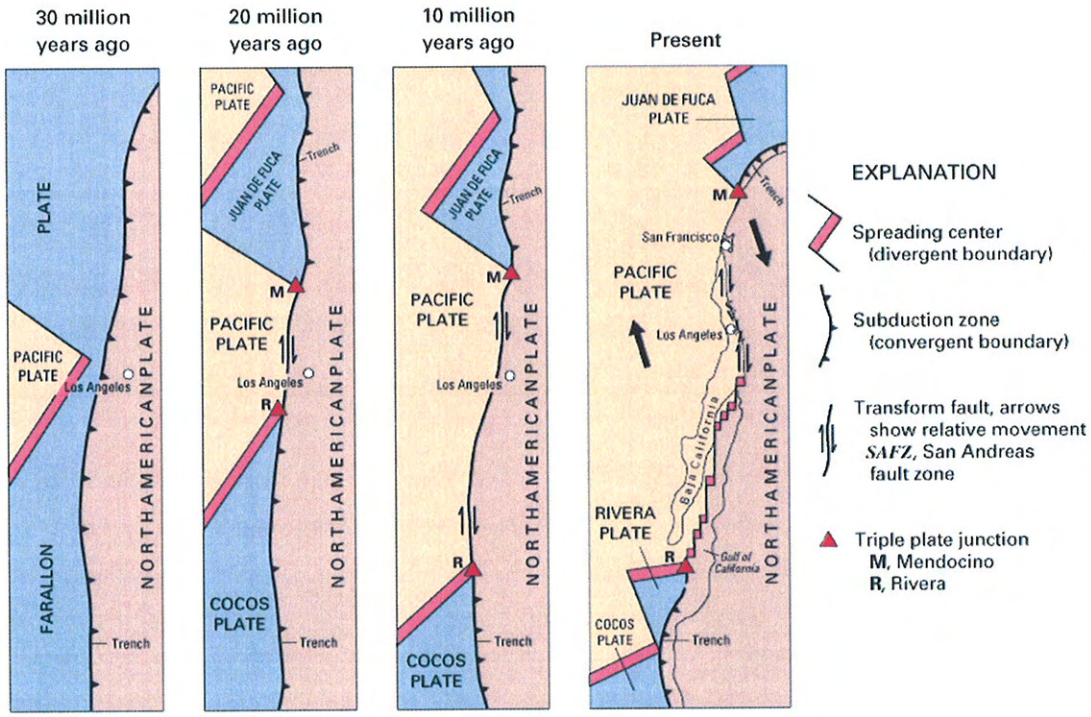

Figure 3. Tectonic setting along the coast of California from Oligocene to present documenting the transition from Andean-type margin to Californian-type margin (www.umt.edu/geosciences/faculty/sheriff; 3/2005).

Stratigraphy

As tectonic events affected the southern San Joaquin basin's structural development, they also affected sedimentation within the basin. The relationship between sedimentation and tectonics was the focus of several stratigraphic studies. These include studies of the stratigraphy and sedimentation of the Eocene Tejon Formation (Nilsen, 1972; Nilsen et al., 1973) and a study of sedimentology and offset along the San Andreas fault (Nilsen and Link, 1975). Bartow (1991, 1992) has done a great deal of work on the stratigraphy and Cenozoic evolution of the valley as a whole. Gorsline and Douglas (1987) analyzed the sedimentary systems within the active margin basins of the California continental borderland. Their study showed the importance of sediment influx rate on the development of basin facies. DeCelles (1988) described the Middle Cenozoic depositional, tectonic, and sea level histories of the southern San Joaquin basin as they are recorded in the strata in the San Emigdio Range that forms the southern margin of the basin

Bent (1988) proposed a paleotectonic and provenance model for Tertiary sandstones of the San Joaquin basin by interpreting petrofacies of formations from Middle Oligocene through Pleistocene time. He concluded that basin evolution centered around three main events: tectonism and volcanism associated with subduction, a change in tectonic regime from convergent to transform resulting in a termination of arc volcanism, and northward migration of the Mendocino triple junction and the subduction zone's southern terminus (Bent, 1988). All of these events are reflected in the stratigraphic and geographic variations of Tertiary sandstones.

Subsidence Modeling

With information gleaned from previous tectonic and stratigraphic studies, basin subsidence models for different regions of the San Joaquin basin have been constructed to further relate tectonics and sedimentation. The locations of some of the major studies are shown in Figure 4. Bandy and Arnal's (1969) research on basin development quantified basin subsidence and uplift based on analysis of foraminiferal faunas from marine Tertiary rocks. Their study showed subsidence occurred everywhere in the San Joaquin basin except for a positive belt extending westward from Bakersfield.

Rentschler and Bloch (1988) numerically modeled subsidence of the central San Joaquin basin, and uplift of the Sierra Nevada, in the Lost Hills area, north of the Maricopa sub-basin. Their study noted that subsidence in the central San Joaquin basin appeared to be caused by loading associated with thrust fault development.

Goodman and Malin (1992) studied the area to the southeast of the Maricopa sub-basin and constructed a geohistory model of the southernmost San Joaquin basin in the Tejon embayment. Their analysis used subsurface data from well bores and seismic data. From this data they constructed a subsidence history that illustrates the relationship between subsidence and time. They related their findings to the nature and timing of major Cenozoic tectonic events and identified five main Oligocene to recent basin phases: Late Oligocene to Early Miocene extensional subsidence, Middle Miocene regional uplift, Late Miocene subsidence to lower bathyal depths, alternating Middle to Late Miocene subsidence and uplift along the San Andreas fault, and subsidence during the Pliocene to recent (Goodman and Malin, 1992).

Preliminary attempts at geohistory modeling were also made by Dickinson et al. (1987), Moxon, (1986) and Olsen et al. (1986). Dickinson et al. (1987) presented a

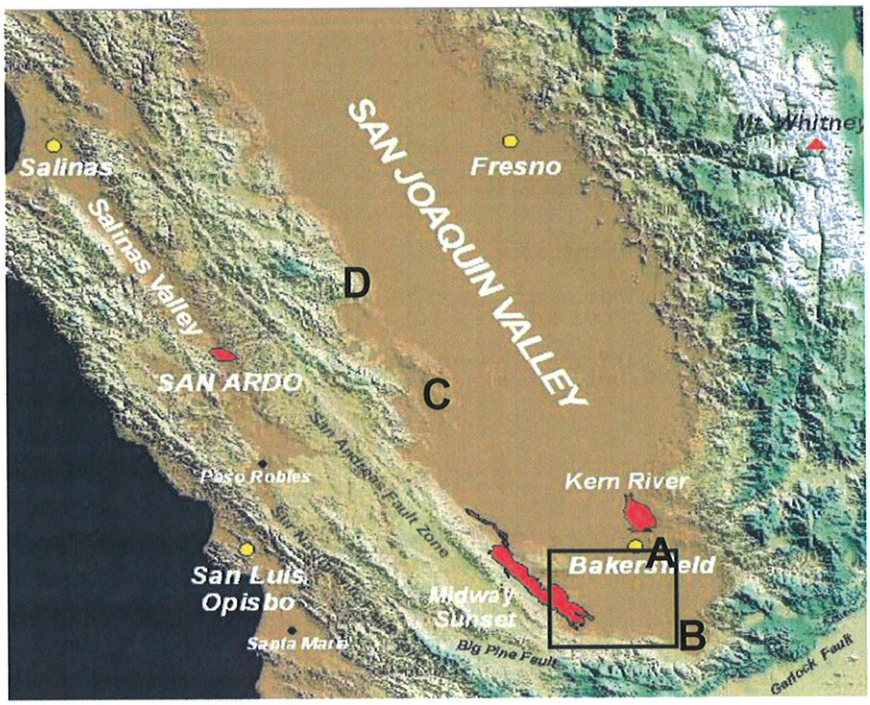

Figure 4. Map of San Joaquin Valley. The boxed area represents the present project area in the Maricopa sub-basin and the letters represent previous geohistory studies in other areas: A) Olsen et al. (1986), B) Goodman and Malin (1992), C) Rentschler and Bloch (1988), D) Dickinson et al. (1987).

partial and approximate geohistory model of the San Joaquin basin from data gathered around Reef Ridge and the Kettleman Hills along the western side of the basin. It was considered an approximate analysis because the authors deliberately restricted the analysis to data that were in the public domain. The data was presented as a guide to improve general concepts of sedimentation relative to tectonics rather than to produce definitive analysis of the tectonic history of sedimentary basins. They concluded that overall sedimentation rates remained constant in the San Joaquin basin and that, for a tectonically active basin, subsidence curves depend critically on paleobathymetry.

Olsen et al. (1986) focused on the stratigraphy, paleoenvironment, and depositional setting of the southeastern San Joaquin basin. Their initial investigation indicated that subsidence curves for the time interval ranging from 40 Ma to 22.5 Ma were compatible with the geohistory pattern of subsidence associated with collision tectonics (Olsen et al., 1986). They also concluded that rapid rates of subsidence at the beginning of Oligocene to Miocene time coincided with the beginning of transform tectonics.

REGIONAL SETTING

Geologic Setting

The San Joaquin basin is bounded on the east by the Sierra Nevada, on the south by the Tehachapi and San Emigdio Mountains, and on the west by the Coast Ranges. It is separated from the Sacramento basin to the north by the Stockton arch (Figure 1).

The San Joaquin basin developed as a forearc basin in the Late Jurassic or Early Cretaceous and was subsequently filled by sediment derived from the Sierra Nevada to the east, the Coast Ranges to the west, and the San Emigdio Mountains to the south (Ingersoll, 1982, 1988; Critelli and Nilsen, 2000). The basin is filled with upper Mesozoic and Cenozoic sediments that are over 9 km thick in the west central and southern end of the basin (Bartow, 1991).

The Maricopa sub-basin lies within the southwestern-most portion of the larger San Joaquin basin. It is bounded to the south by the San Emigdio Mountains and to the west by the Coast Ranges. To the north the Bakersfield arch separates the Maricopa sub-basin from the rest of the San Joaquin basin. The Maricopa sub-basin is separated from the shallower Tejon Embayment by the White Wolf fault. Figure 5 illustrates the relationships between the Maricopa sub-basin and the Tejon embayment as well as some of the surrounding major oil fields in the area.

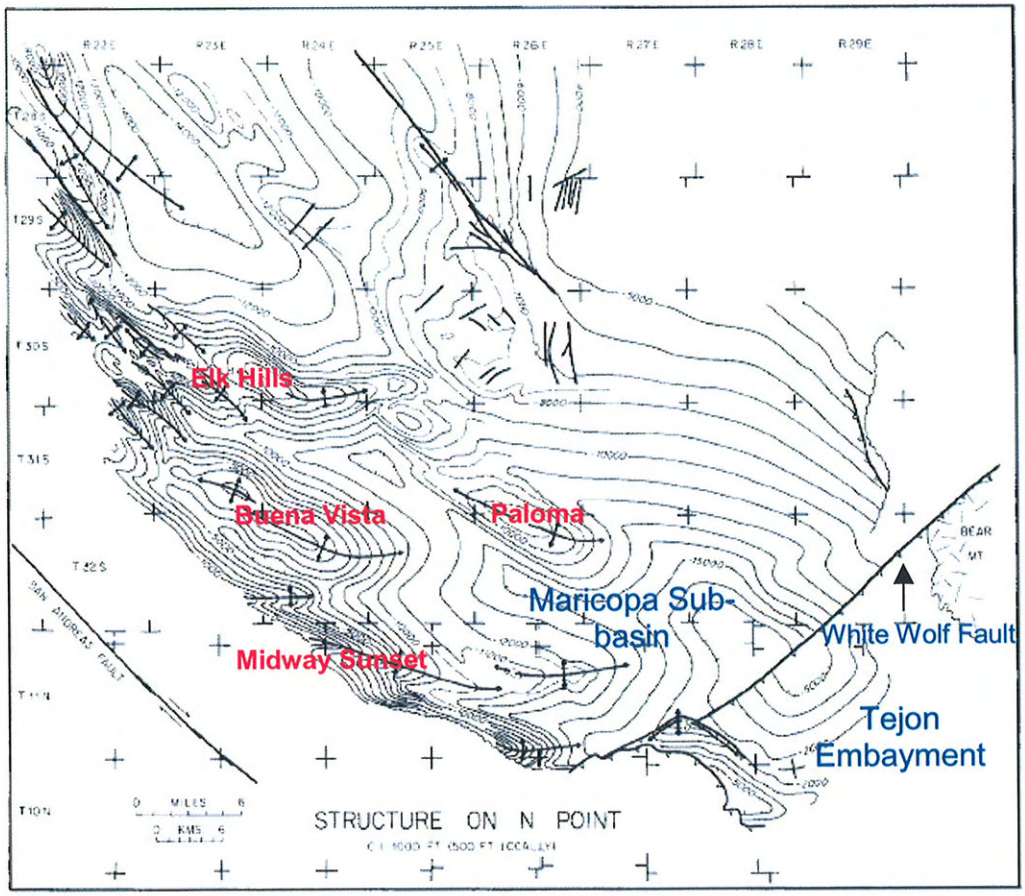

Figure 5. Structure Map on N point marker near top of upper Miocene, showing relationship between Tejon Embayment and Maricopa sub-basin. Major oil fields are labeled in red (Modified from Webb, 1981).

Tectonic Setting

The San Joaquin and Sacramento basins make up the Great Valley forearc basin that formed during the subduction of the ancestral Farallon plate beneath the North American plate during the Jurassic to Eocene (~181-60 Ma). During the Oligocene California underwent a significant tectonic transition between what Dickinson (1987) described as an Andean-type margin to a Californian-type margin. The Andean-type margin was characterized by subduction of oceanic crust beneath continental crust in a

manner similar to the west coast of present-day South America. As the Farallon plate was subducted beneath the North American plate to the east (Figure 3), the spreading center of the East Pacific Rise drew closer to the subduction zone (Bartow, 1991).

During Middle Oligocene time (28-30 Ma), the East Pacific Rise encountered the trench and the Pacific plate came into direct contact with the North American plate marking the beginning of transform motion along the plate boundary (Bartow, 1991; Atwater and Molnar, 1973; Engebretson and others, 1985). This sequence of events created the Mendocino triple junction and the Riviera triple junction at the north and south ends of the San Andreas fault respectively. As the Mendocino triple junction migrated north along the western margin of the San Joaquin basin, the San Andreas fault evolved and lengthened. The San Andreas fault system presently separates the San Joaquin basin on the North American plate from rocks of the Coast Ranges on the Pacific plate to the west (Bent, 1988).

BASIN HISTORY

The transition from convergent to transform plate boundaries along the western margin of the San Joaquin basin influenced the Maricopa sub-basin's evolution, eventually making it one of the deepest and most deformed regions in the San Joaquin basin. The basin evolution of both the San Joaquin basin and Maricopa sub-basin will be discussed for each plate boundary setting: convergent, transitional, and transform.

Convergent Plate Boundary

The San Joaquin basin is a composite of a Late Mesozoic and Early Cenozoic forearc basin, largely open to the Pacific Ocean to the west, and a more restricted Late Cenozoic transform-margin basin. According to Dickinson (1987), an Andean-type plate margin persisted from Late Triassic to Oligocene time. During that time, the Great Valley formed as a forearc basin with the Sierra Nevada magmatic arc to the east as part of an arc-trench system. Sediment was fed into the basin from the Klamath Mountains to the north and the Sierra Nevada to the east (Ingersoll, 1978, 1979, 1982, 1988).

Paleogene basin history was controlled principally by subduction related to the proto-San Andreas fault and, to a lesser extent, the effects of eustatic sea level (Bartow, 1991). During the Paleocene, the principal factors influencing the paleogeography were right slip on the proto-San Andreas fault, causing uplift of the Stockton arch, and a north-south compressive stress on the region. Figure 6 shows the paleogeography of the area during Early Eocene time as the basic arc-trench system persisted but began to be affected by right-lateral motion on the proto-San Andreas fault. The San Joaquin basin became separated from the Sacramento basin to the north as the Stockton arch became

emergent. Sediment source terrains included the Coast Ranges to the west as well as the San Emigdio Mountains to the south near the end of the Eocene.

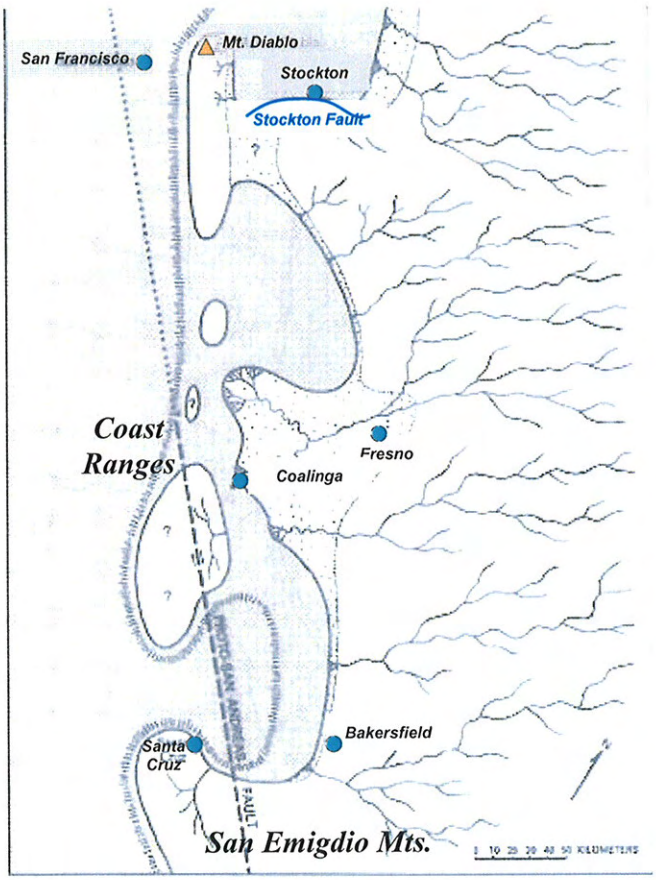

Figure 6. Paleogeography during the Early Eocene (~52Ma) modified from Bartow (1991). Note the emergence of the Stockton arch separating the San Joaquin basin from the Sacramento basin to the north. Based on data from Repenning (1960), Clarke et al (1975), Graham (1978), Graham and Berry (1979), Nilsen (1979), Nilsen and McKee (1979), Slagle (1979), and Stanley (1985).

Transitional Plate Boundary

A major change in tectonics took place during the Oligocene when the East Pacific Rise spreading center collided with the western continental margin of North America (Atwater and Molnar, 1973). This resulted in the formation of the San Andreas fault system and the transition of the western margin from convergent tectonics to transform tectonics. During the Oligocene, the San Joaquin basin changed from a west facing continental slope to an asymmetrical, semi-closed basin (Davis and Lagoe, 1988). This, combined with eustatic sea level change, produced major changes in central California basin evolution (Bartow, 1991). In the Stockton arch to the north and the San Emigdio area in the south, uplift continued (Bartow, 1991).

The Stockton arch developed by northward-directed thrusting during the latest Eocene to Early Oligocene (Erskine, 1992). This gave the basin a slight southward tilt and caused the northern part of the basin to become emergent. The semi-closed basin was caused by the continued tectonic uplift of the Diablo and northern Temblor Ranges along the west side of the basin during the Oligocene (Figure 7). The basin became closed off from the Pacific Ocean except for a narrow seaway at the southern end of the basin.

During the Oligocene, the southwestern San Joaquin basin's paleobathymetry was characterized by abyssal depths adjacent to strongly positive areas (Figure 7). Deeper areas existed north of Bakersfield and in the southwest region of the basin. Bandy and Arnal's (1969) Oligocene (Zemorrian) paleotectonism map (Figure 8) shows subsidence occurred everywhere in the San Joaquin basin except in a positive belt extending westward from Bakersfield in the location of the present day Bakersfield arch. This indicates the Bakersfield arch may have been present as early as Oligocene time.

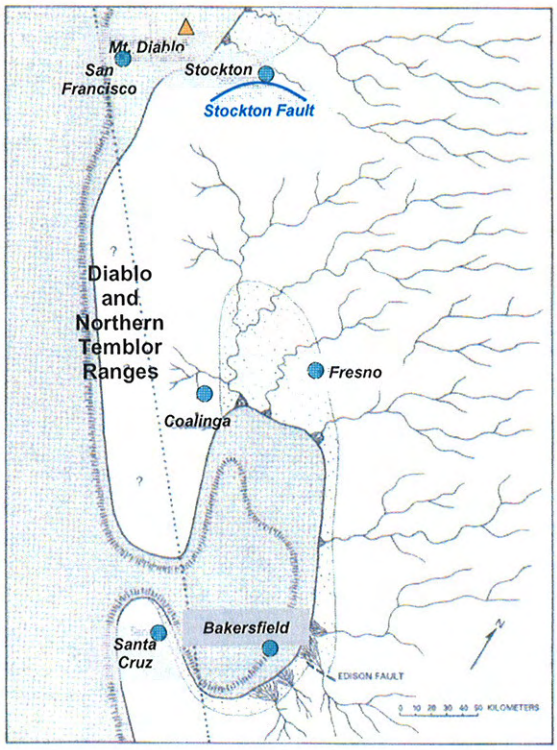

Figure 7. Oligocene (about 30 Ma) paleogeography of the San Joaquin area modified from Bartow (1991). Based on data from Repenning (1960), Addicott (1968), Bandy and Arnal (1969), Greene and Clark (1979), Nilsen and McKee (1979), Nilsen (1984), and Pence (1985).

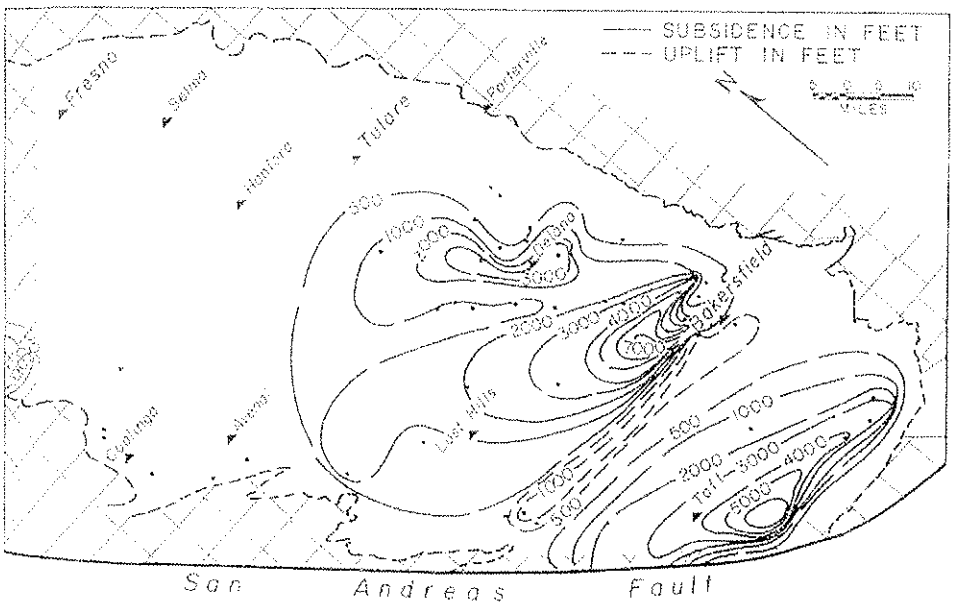

Figure 8. Paleotectonic map for the Zemorrian stage, San Joaquin basin, with isopleths of vertical movement in feet. Uplift is represented by dashed lines (Bandy, O.L. and Arnal, R.E., 1969).

Transform Plate Boundary

The current transform plate boundary formed during the Neogene (Dickinson, 1987) as the passage of the Mendocino triple junction along the western margin of the San Joaquin basin created and lengthened the San Andreas fault system. Neogene basin history was controlled principally by the tectonic effects of the northwestward migration of the Mendocino triple junction along the California continental margin and by the subsequent wrench tectonism associated with the San Andreas fault system.

Overall, the tectonic history of the basin during Neogene time can be summarized as alternating periods of compression and extension in a north-south direction. Patterns of regional-stress change began at the southernmost end of the basin where east-west

oriented normal faulting, along with basin subsidence, indicate north-south extension (Bartow, 1991). With the northward migration of the Mendocino triple junction during Miocene time, the paleogeography changed significantly as uplift of the southern part of the basin produced a sea-level regression and caused alluvial-fan and fan-delta deposits to prograde basinward from the east (Bartow, 1991). Marine deposition was restricted to the southwestern part of the basin.

Paleobathymetric depths recorded in the Middle Tertiary deposits of the Maricopa sub-basin are the deepest found in the San Joaquin basin (Bartow, 1991). According to Bandy and Arnal (1969), abyssal depths (1800 m) were reached in the Zemorrian, Saucesian and Luisian stages (Oligocene through Middle Miocene). The basin gradually became shallower through the Late Neogene and became entirely non-marine during Late Pliocene time (Bartow, 1991).

During the Late Cenozoic, there was a change in relative plate motion between the North American and Pacific plates as the Pacific plate changed to a more northerly overall plate motion (Page and Engebretson 1984; Engebretson et al., 1985). This caused compression normal to the San Andreas fault and contributed to compressional deformation on the west side of the valley. Thrust faulting along the western margin of the basin resulted in several kilometers of crustal shortening (Davis, 1983). Also, wrench tectonics in conjunction with deep-seated thrusting along the southwestern side of the basin adjacent to the San Andreas fault dominated the Neogene. This caused the southwestern end of the San Joaquin basin to be the most highly deformed region in the basin (Bartow, 1991).

STRATIGRAPHY OF THE MARICOPA SUB-BASIN

The Maricopa sub-basin contains some of the thickest and most complete Cenozoic deposits in the San Joaquin basin. The sedimentary history of the San Joaquin basin was controlled principally by tectonism although eustatic sea level change also played a part (Bartow, 1991). This is recorded in the strata deposited during this period. For the present study five main stratigraphic units were used in constructing the geohistory models. These are the Monterey, Reef Ridge, Etchegoin, San Joaquin, and Tulare Formations. Figure 9 is a general stratigraphic column for the southwestern San Joaquin basin.

Monterey Formation

The Monterey Formation is Middle to Late Miocene in age (Maher et al., 1975) and was the first geologic formation to be described in California. This unit is up to 2,500 feet thick (Graham and Williams, 1985) and is characterized by medium-brown, cherty, diatomaceous shale, organic siliceous shale, and diatomite (Reid, 1995).

It was deposited in a deep-water setting after wrench tectonism had produced a complex sea floor similar to that of the current California borderland (Graham et al., 1982; Reid and McIntyre, 2001). By Late Miocene the emergent highlands to the west of the basin combined with the deep-marine setting within the basin to create an ideal environment for the preservation of organic-rich, diatomaceous rock (Graham and Williams, 1985; Reid and McIntyre, 2001). Sand-rich sediment, sourced from the highlands to the west and south, was deposited in the basin creating submarine fans that prograded across the deep floor of the basin (MacPherson, 1978; Webb, 1981).

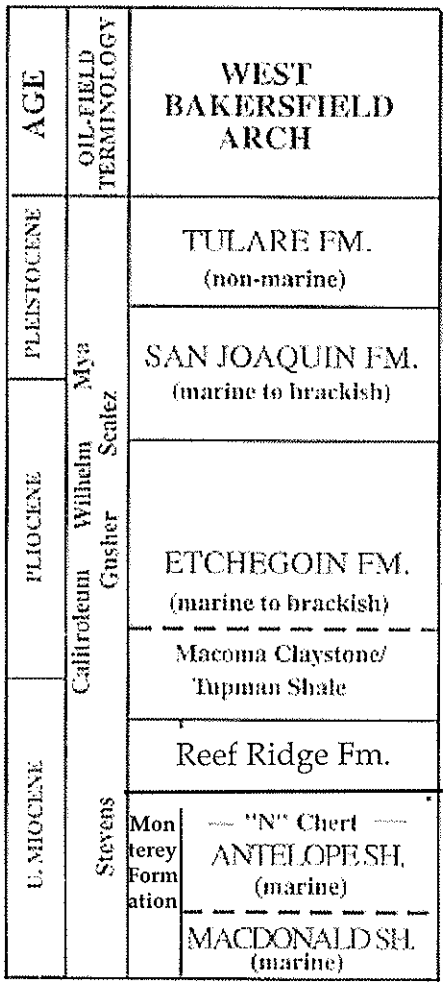

Figure 9. Stratigraphy of the western Bakersfield arch. The 'N' Chert is a widely mapped marker bed within the upper Antelope Shale (Jones and Gillespie, 1997). The 'N' Chert was the marker bed used in the structure map in Figure 5.

Reef Ridge Formation

The Reef Ridge Formation was deposited in Late Miocene time (10-5 Ma). It varies in thickness from 0-5,000 ft in the study area and was first defined by Barbat and Johnson (1934) and later modified by Seigfus (1934). The unit is characterized by light to dark gray-brown, fine-grained, well sorted sand that grades into siliceous shale near the base of the formation.

The sediments of the Reef Ridge Formation were deposited as coalesced turbidite fans in deep-marine settings or as channel sands on the proximal portion of submarine-fan complexes (Fedewa and Simmons, 1997). The sediment source for the Reef Ridge Formation was the highlands to the west and south of the basin.

Etchegoin Formation

The Upper Miocene to Pliocene (5-3.5 Ma) Etchegoin Formation contains a thick series of sediments that unconformably overlie Upper Miocene sands and siliceous shales of the Reef Ridge Formation (Barbat and Johnson, 1934). Pierce (1949) reported thickness variations of 1,000-3,500 feet for the Etchegoin Formation in the study area. The Etchegoin Formation is characterized by alternating bluish-gray to green, diatomaceous, and micaceous claystones, and tan siltstones (Peirce, 1949). Lower in the section there are dark-brown, oil-stained, medium-grained, massive, pebbly sands.

The sediments of the Etchegoin Formation were deposited in a shallow-marine setting. During this time, alluvial fans formed at the base of the Sierra Nevada and transitioned into braided streams basinward. As the slope decreased, a mud-rich coastal plain extended to the shoreline on a marine embayment (Link et al., 1990). The sandstone and conglomerate lithofacies of the Etchegoin Formation are interpreted to be

fluvial channel deposits, formed on a mud-rich coastal plain, and narrow linear deltaic sequences that consist of mouth bar deposits (Link et al., 1990). The mudstones and sandstones are interpreted to be marine to prodelta deposits that were subject to reworking by organisms and by rapid fluvial or deltaic sediment influxes (Link et al., 1990).

San Joaquin Formation

The San Joaquin Formation was deposited from the Late Pliocene to Early Pleistocene (3.5-2 Ma). It is characterized by interbedded, massive claystone, and gray, fine- to coarse-grained sands. The lower section of the San Joaquin Formation contains fine- to coarse-grained oil sands with interbedded siltstones.

During the deposition of the San Joaquin Formation, the seaway connection between the Pacific Ocean and the San Joaquin basin became even more restricted as sea level decreased. This restricted the marine deposits of the San Joaquin Formation to the central region of the basin and caused fluvial and deltaic floodplain depositional environments to prevail in the north and south parts of the basin (Loomis, 1990). The sand deposits of the San Joaquin Formation consist of detritus from the dissected Sierran magmatic arc to the east and the Coast Ranges to the west of the San Andreas fault (Loomis, 1990).

Tulare Formation

The Tulare Formation is separated from the underlying San Joaquin Formation by an unconformity and was deposited during Late Pleistocene time (Pierce, 1949). The Tulare Formation and overlying alluvium range from 1,250 to 5,000 feet in thickness

throughout the study area. The 5,000 feet of sediment thickness in the eastern edge of the study area is consistent with the California Department of Oil Gas and Geothermal Resources reports on oil fields within this area. The Tulare Formation consists mainly of clays and conglomeratic sands in the uppermost portion and massive, light-gray to blue-green claystone, and poorly sorted siltstone in the lower portion (Pierce, 1949). Oil is produced from sands in the lower part of the section. These oil sands are characterized as medium brown, friable, fine to coarse grained, fairly well-sorted, oil sand interbedded with claystone.

The overall depositional setting of the Tulare Formation was that of a prograding fluviodeltaic system that included lacustrine, deltaic, and meandering and braided fluvial systems (McPherson and Miller, 1990). The prograding, fluviodeltaic depositional system was influenced by source area tectonics and basinal subsidence rates (McPherson and Miller, 1990). The lower Tulare sands are mostly of delta-front origin with some distal bar and channel sands, while the upper Tulare sands are fluvial and consist of meander belt sands and fluvial braided sands (McPherson and Miller, 1990). The sediment source for the Tulare Formation was the Temblor Range to the west of the basin and the Sierra Nevada to the east of the basin.

DATA AND METHODS

Several types of data were needed in order to create the geohistory analyses and isopach maps for the Maricopa sub-basin. For the geohistory analysis, the required data included stratigraphic thicknesses of each unit, type of lithology, ages of each horizon, and estimated paleowater depth. Constructing the isochore maps required stratigraphic thicknesses for each unit based on well log data from 130 wells within the study area (Figure 10). A list recording each well used in the project is located in the Appendix with their corresponding ID, location, total depth, and depth of each pick.

The deepest wells in each township and range within the study area were selected using the Access database provided by the California Department of Oil, Gas and Geothermal Resources (DOGGR) and from California Summary of Operations books for individual oil fields. Data from Petroleum Information and Dwights software provided by the California Well Sample Repository at the California State University, Bakersfield (CSUB) campus were also used. Copies of all logs were obtained from the Department of Oil, Gas and Geothermal Resources, the California Well Sample Repository and from well log collections in the Geology Department at CSUB.

All well logs were interpreted in order to determine the stratigraphic thicknesses of five units: the Tulare, San Joaquin, Etchegoin, Reef Ridge, and Monterey Formations. Some well logs did not penetrate to the base of the Monterey Formation so only the thicknesses of the Antelope Shale Member of the Monterey Formation were recorded. Stratigraphic picks for the tops of these units were made based on type logs provided by CSUB and by type logs published by the DOGGR Summary of Operations. Figure 11 is an example of a type log used in the project.

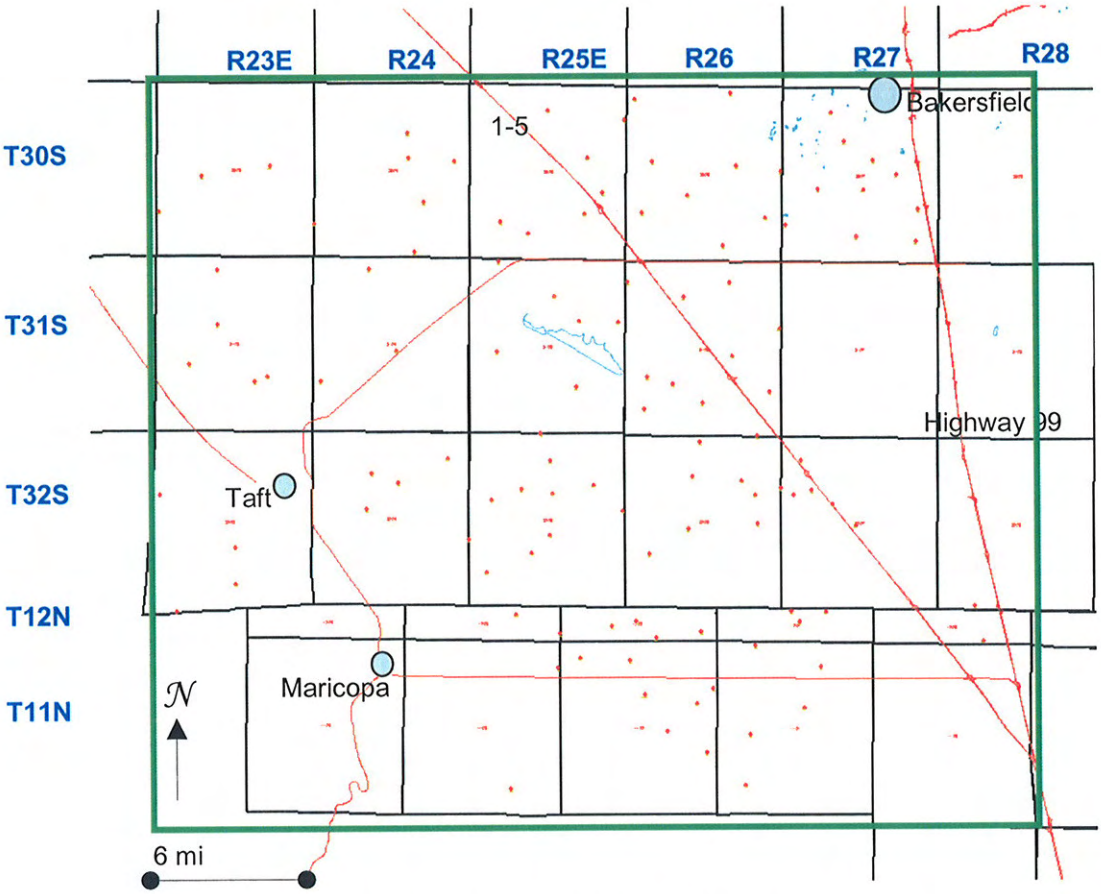

Figure 10. Green indicates outline of project area with red dots indicating locations of all wells within the project area. Blue dots represent general location of cities. This map gives a general indication of well distribution used for creating each isopach map. Appendix A is a list of all the wells within the project area outlined.

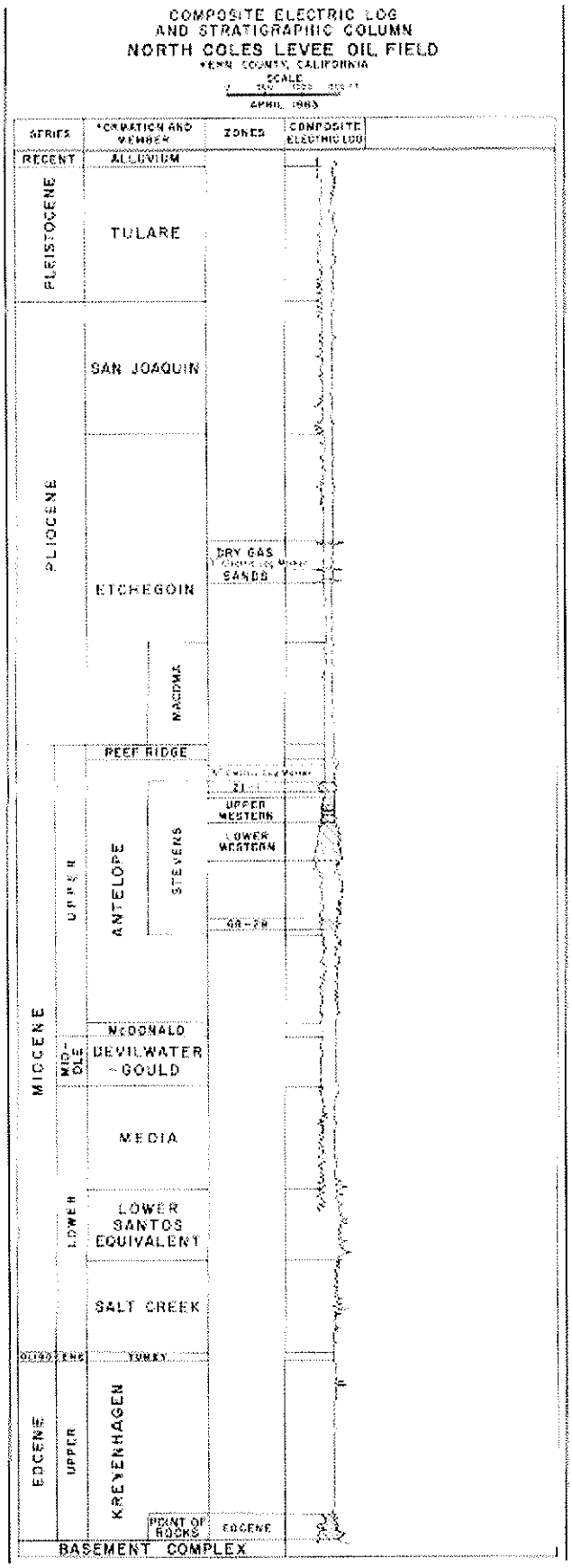

Figure 11. Type Log of North Coles Levee oil field, from Hardoin (1962). This type log was used to make picks for each of the major formations.

The measured depth to each stratigraphic pick in each well was entered into GeoGraphix software and isochore maps were constructed for the Reef Ridge, Etchegoin, San Joaquin, and the Tulare Formations. The isochore maps were created in order to determine the thickness distribution of each unit throughout the Maricopa sub-basin and to understand how the geohistory models may vary away from the three wells used to create them. Since a geohistory model is created from data taken from a single point, the isochore maps illustrate lateral thickness variations within each unit to help determine how representative the geohistory models are of the three locations within the sub-basin.

Data for lithology and ages of each unit, as well as paleowater depths, were obtained from published reports (Bartow, 1992). Lithology for each unit was estimated based on the lithologic descriptions from Pierce (1949). Ages of each horizon in the region of the Maricopa sub-basin were based on Bartow's (1991) synthesis of the evolution of the San Joaquin basin. In order to remain consistent with the methods and data used by Goodman and Malin (1992) in constructing the geohistory model, the paleo-sea-level data was derived from Haq et al's (1987) analysis of sea-level fluctuation since the Triassic.

Using the unit thickness, lithology, age, and paleobathymetry data, geohistory models were constructed for three locations within the Maricopa sub-basin using BasinMod 1D software from Platte River Associates in order to model the evolution of each location individually. Figure 3 shows the locations of each of the wells used in the geohistory analyses.

The Cerrina #1-32 well was drilled in 1980 in section 32 of T32S R28E. The upper Miocene sediments of the Monterey Formation were encountered at the total depth

of 17,802 feet. This well was used in Goodman and Malin's (1992) study and represents the southeastern portion of the study area. This well also was used in this study to recreate Goodman and Malin's (1992) analysis and to expand their methods to the northwest across the Maricopa sub-basin.

Well # KCL-A 72-4 in section 4 of T32S R26E in the Paloma oil field was used to analyze the center of the Maricopa sub-basin. This well was drilled in 1952 to a depth of 21,482 feet and reached strata of the Early Miocene age Santos Formation lying below the Monterey Formation. The northwestern edge of the study area is represented by well # 987-25R in section 25 of T30S R23E in the Elk Hills oil field. This well was drilled in 1977 to a depth of 18,761 feet into Early Miocene sediments of the Santos Formation. Each geohistory model consists of three curves: the top curve graphically represents paleobathymetry of the basin through time, the middle curve represents subsidence within the basin due to tectonic effects and the bottom curve represents total subsidence as a result of sediment loading as well as tectonic effects.

RESULTS AND DISCUSSION

The goal of a geohistory analysis is to produce a graphical presentation of the vertical movement of a stratigraphic horizon in a sedimentary basin over time. This provides a model of subsidence and uplift history in the basin that occurred after the horizon was deposited (Van Hinte, 1978). The three geohistory models created for this project show how the Maricopa sub-basin evolved through time as regional plate tectonic regimes changed. The geohistory models generated for the project were compared to the model created by Goodman and Malin (1992) for the Tejon embayment region to the southeast of the study area and Rentschler and Bloch's (1988) analysis near Lost Hills, California along the western flank of the Temblor Ranges to the north of the study area.

Isochore Maps

The isochore maps created for the Tulare, San Joaquin, Etchegoin, and Reef Ridge Formations are shown in Figures 12-15. These were created in order to 1) determine thickness trends of the individual units within the Maricopa sub-basin region and 2) determine whether the geohistory models in this report are representative of their location in the basin or if they represent areas of anomalous thickness.

The isochore map of the Late Miocene (9-5 Ma) Reef Ridge Formation (Figure 12) shows the sediments thickening in the west-central area of the sub-basin between the Elk Hills and Paloma oil fields. Here the sediments are ~5000 feet thick and indicate subsidence of the basin took place in this area at the time of deposition. The isochore map also shows a gradual thinning of sediments to the east as well as southwest areas of the sub-basin, indicating a relatively lower degree of subsidence in these areas.

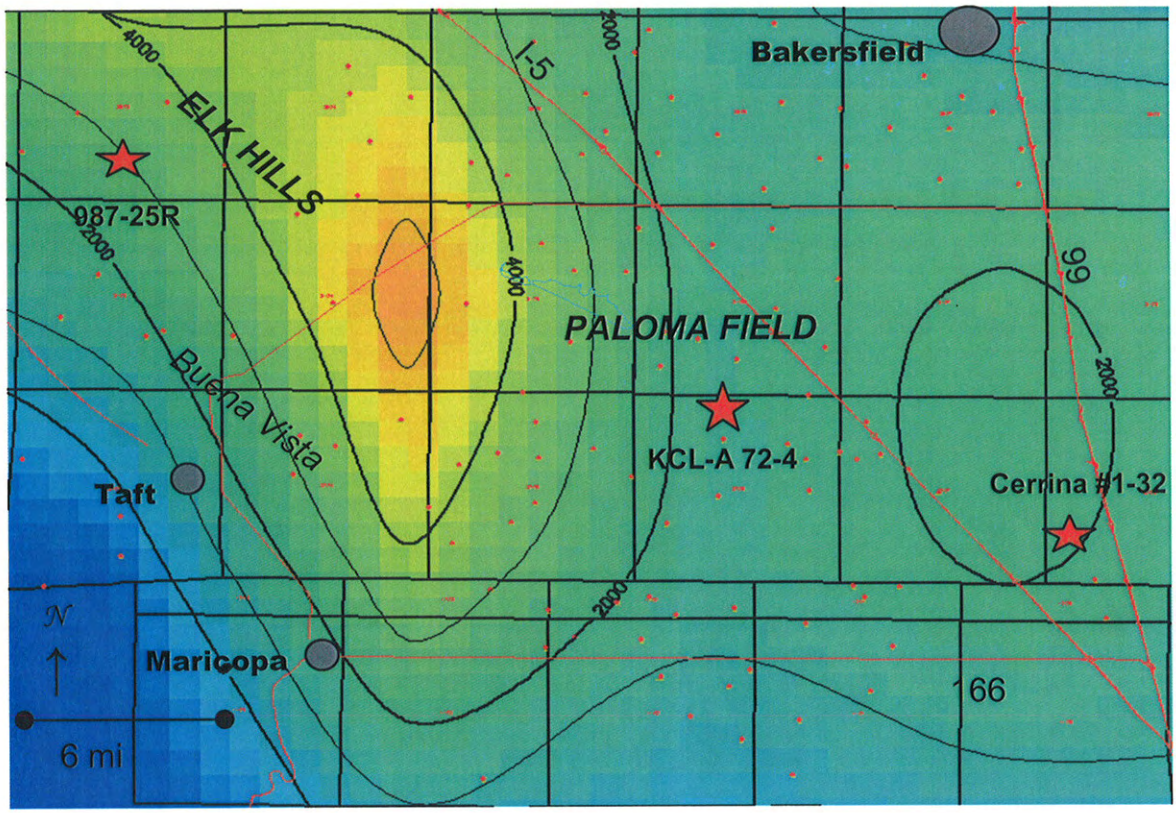

Figure 12.

Isochore Map of Reef Ridge Formation (9-5 Ma). Blue shading indicates area of non deposition or deposition and subsequent erosion; red shading indicates areas of thicker sediment. Red dots represent locations of wells which were used to create isochore maps. Black boxes outline township and ranges within the project area. The wells used to create the geohistory analyses for the Maricopa sub-basin indicated by a red star. Gray circles represent location of nearby cities. Note the area of thicker sediment accumulation in the west-center of the study area. CI=1000'

Thicknesses in these areas range from ~2000 to 3000 feet. In the far southwest corner, to the southwest of Maricopa and Taft, the Reef Ridge Formation is absent.

The isochore map of the Etchegoin Formation (Figure 13) represents sediments deposited in Early Pliocene time (5-3.5 Ma). The isochore map of the Etchegoin Formation shows a region between Elk Hills and Paloma oil fields where the sediments are thicker than elsewhere in the basin. This suggests localized subsidence in the area during deposition. There is a small region in the southwestern region of the sub-basin near the town of Maricopa where the sediments become thinner. This suggests uplift resulted in erosion of the Etchegoin Formation in this area. The isochore map of the Etchegoin Formation does show other localized areas of thickening and thinning of sediment suggesting localized areas of uplift and subsidence within the sub-basin.

The isochore map of the San Joaquin Formation (Figure 14) represents sediments deposited in Late Pliocene time (3.5-2 Ma). Thicker sediments are located in the southwestern-most region of the sub-basin and become thinner towards the northwestern and northeastern portions of the sub-basin. The isochore map also shows the sediments are thinner along the entire western side of the sub-basin indicating non-deposition or deposition and subsequent erosion of the San Joaquin Formation.

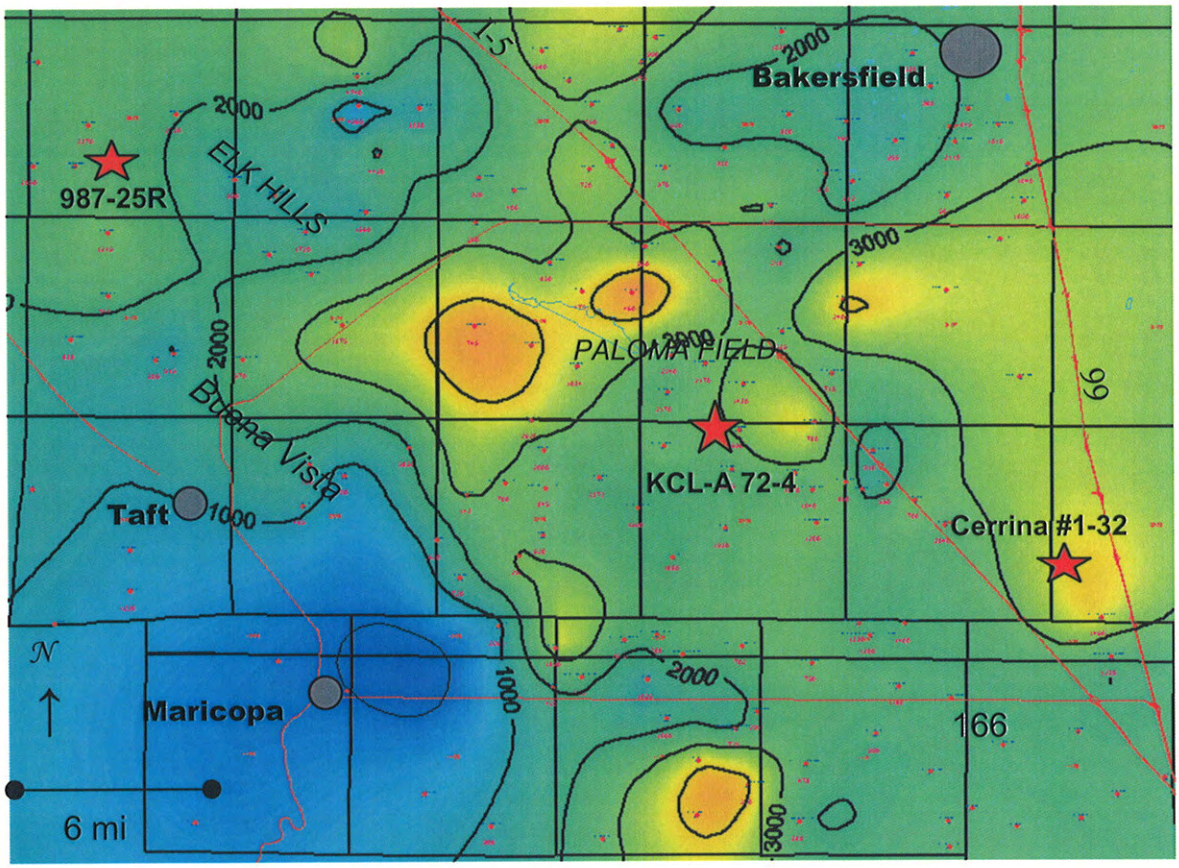

Figure 13.

Isochore Map of Etchegoin Formation (5-3.5 Ma)
Blue shading indicates area of non deposition or deposition and subsequent erosion; red shading indicates areas of thicker sediment. Red dots represent locations of wells which were used to create isochore maps. Black boxes outline township and ranges within the project area. The wells used to create the geohistory analyses for the Maricopa sub-basin indicated by a red star. Gray circles represent location of nearby cities. Note the area of thinning sediments in the western portion of the basin. This represents an area where the Etchegoin Formation was not deposited or deposited and then eroded due to uplift. CI=1000'

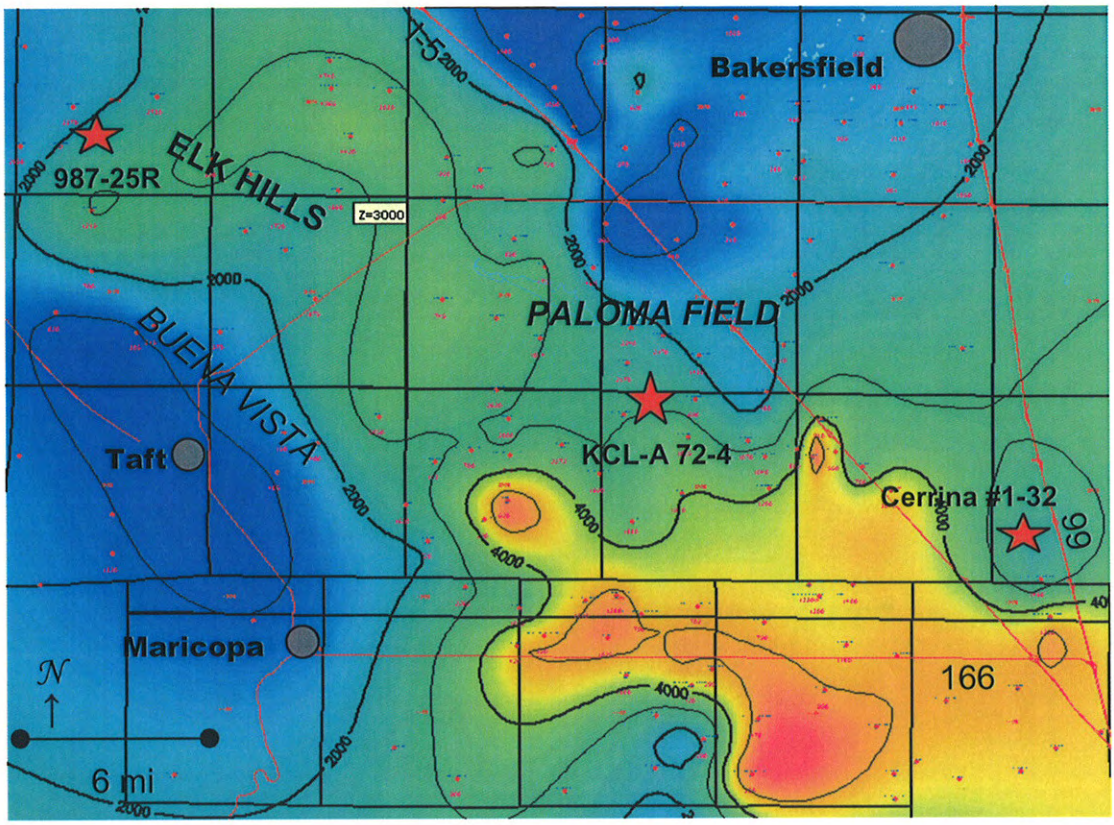

Figure 14.

Isochore Map of San Joaquin Formation (3.5-2 Ma). Blue shading indicates area of non deposition or deposition and subsequent erosion; red shading indicates areas of thicker sediment. Red dots represent locations of wells which were used to create isochore maps. Black boxes outline township and ranges within the project area. The wells used to create the geohistory analyses for the Maricopa sub-basin indicated by a red star. Gray circles represent location of nearby cities. Deposition of the San Joaquin Formation occurred at a constant rate throughout the central portion of the basin. This is represented by the region of green shading which indicates a similar thickness of the strata.
CI=1000'

The Tulare Formation and alluvium isochore map (Figure 15) represents sediments deposited during Pleistocene and Holocene time (2-0 Ma). The isopach map shows a sedimentary prism that thickens eastward within the project area and becomes thinner to the west. The thicker sediments indicate a higher rate of sediment input or a higher rate of subsidence as the basin subsequently filled with sediment. The thinner sediments to the west indicate a decrease in subsidence relative to the eastern portion of the sub-basin or an episode of uplift and subsequent erosion of the sediments.

Based on the isochore maps the locations of the geohistory models created for the Maricopa sub-basin are adequate for creating a generalized picture of subsidence for the region. The three wells used in the geohistory analyses are located in regions of the basin that are not characterized by anomalous thickness values on the isochore maps.

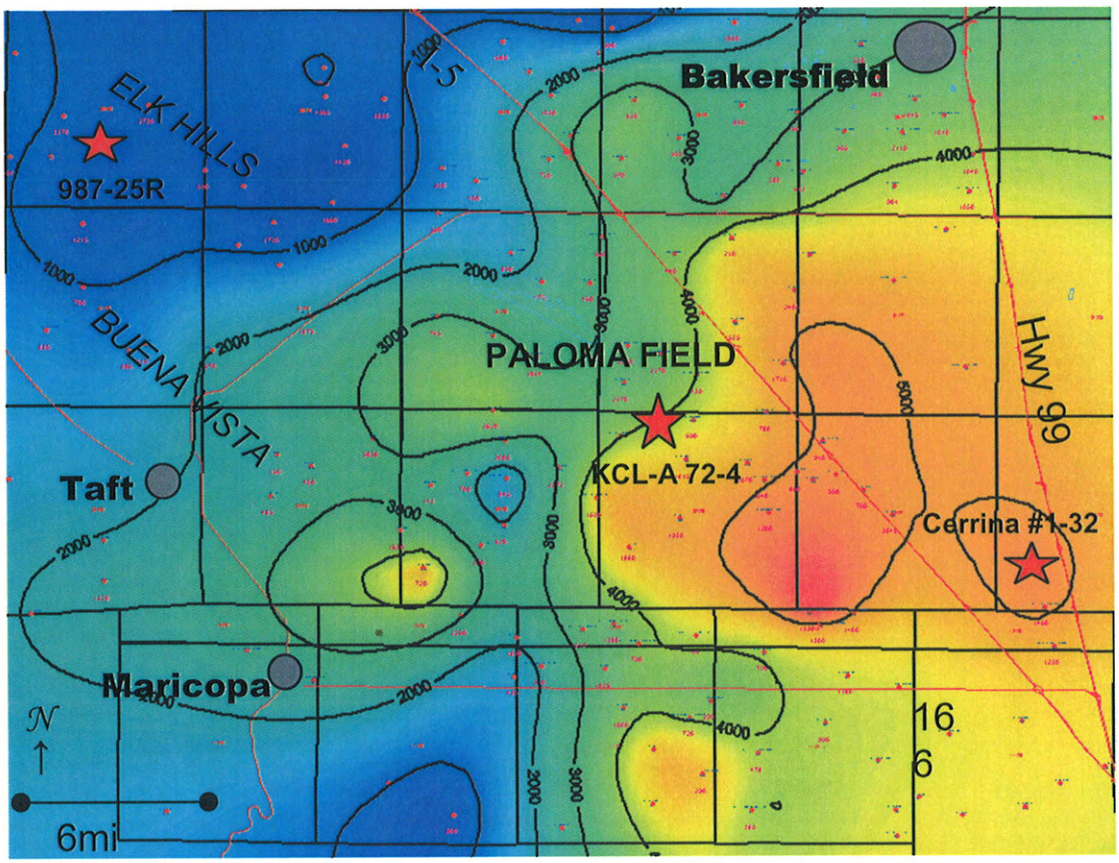

Figure 15.

Isochore Map of Tulare Formation and Alluvium (2.5-0 Ma). Blue shading indicates area of non deposition or deposition and subsequent erosion; red shading indicates areas of thicker sediment. Red dots represent locations of wells which were used to create isochore maps. Black boxes outline township and ranges within the project area. The wells used to create the geohistory analyses for the Maricopa sub-basin are indicated by a red star. Gray circles represent location of nearby cities. Note the general trend of sediment thickening to the east and thinning to the west. CI=1000'

Cerrina Well # 1-32 Geohistory Model

The Cerrina #1-32 well is located in the eastern Maricopa sub-basin. The geohistory model generated for this well is shown in Figure 16. The well penetrates Late Miocene age sediments at total depth and therefore the geohistory model curves begin at 15 Ma. The middle curve represents subsidence due to tectonism. The bottom curve in the diagram represents total subsidence of the basin and takes into account subsidence due to tectonism as well as sediment loading.

The geohistory model shows the basin underwent rapid subsidence from 15-12 Ma due primarily to tectonic loading. This is illustrated by the tectonic subsidence curve plotting very close to the total subsidence curve. The geohistory model shows an abrupt change at 12 Ma indicating an episode of uplift and marine regression. Subsidence then occurred from 11 Ma to the present with an increase in the subsidence rate at 2 Ma. The model suggests sediment loading was the principle mechanism for subsidence during this time.

The Cerrina #1-32 is the same well used in Goodman and Malin's (1992) study of the Maricopa sub-basin. Their geohistory model is shown in Figure 17. The geohistory model constructed for this study shows the same general shape as their geohistory model and therefore indicates that the data and methodology are consistent and can be applied to create geohistory models in other areas of the basin.

A slight discrepancy exists in the timing of events between the two models as well as the time each model represents. This could be due the differing age data used in the two studies. Goodman and Malin (1992) used biostratigraphic markers to create their

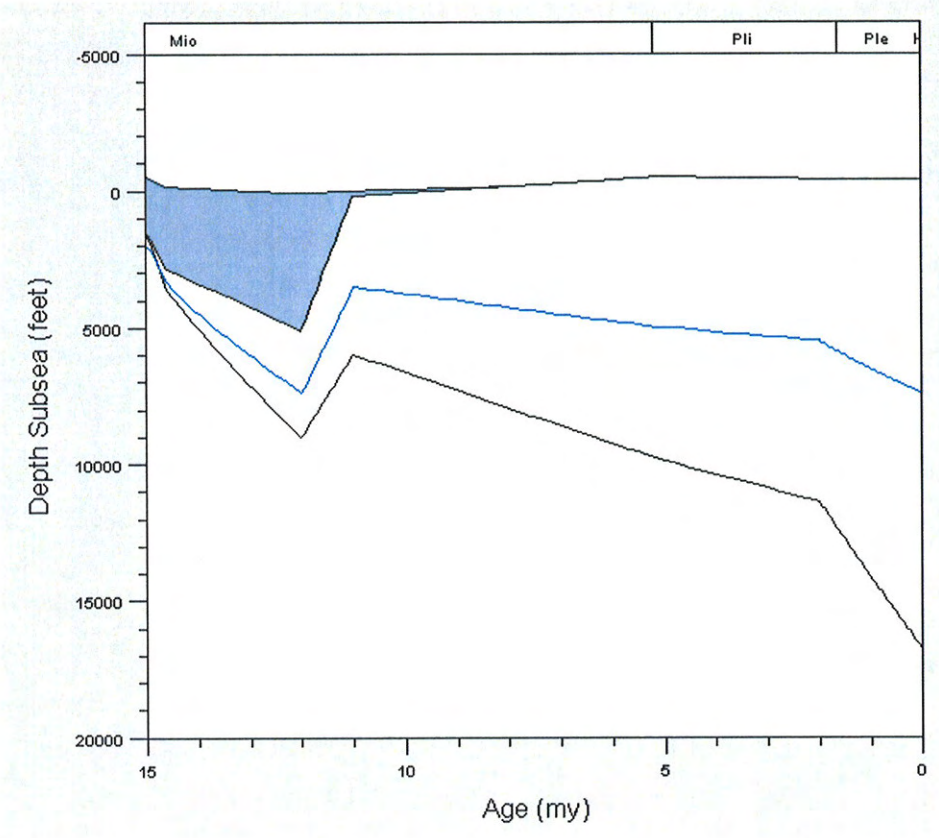

Figure 16. Geohistory model for the Cerrina well #1-32 in the southeasternmost portion of the project area. Blue shaded area represents paleobathymetry with the top curve representing paleo sea level and surface elevation. The middle (blue) curve represents subsidence due to tectonism and the bottom curve represents total subsidence due to tectonism as well as sediment loading. The general concave down shape suggests thrust loading as a mechanism for basin subsidence (Rentschler and Bloch, 1988). The horizon tracked is the deepest horizon this well penetrates which is the Stevens sand Member of the Monterey Formation. Mio=Miocene; Pli=Pliocene; Ple=Pleistocene.

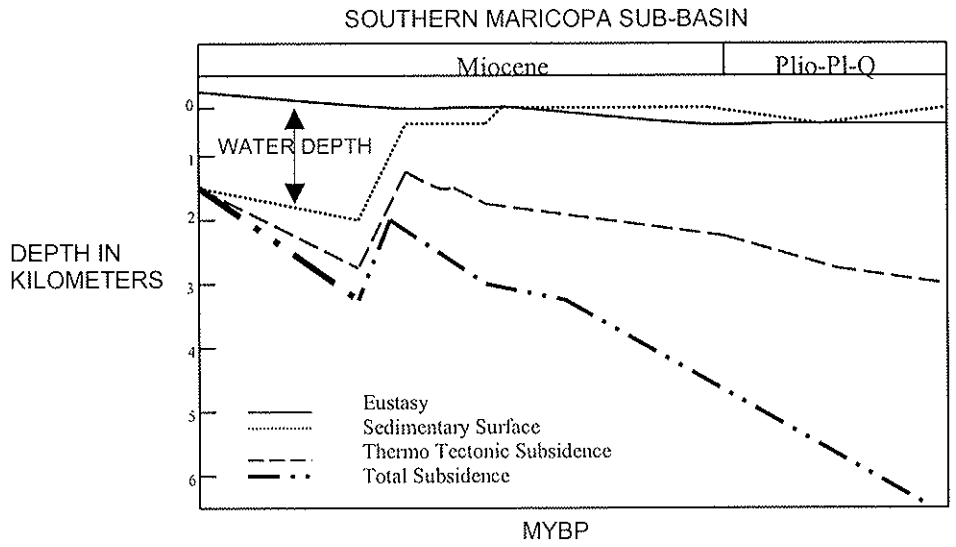

Figure 17. Geohistory model for the southern Maricopa sub-basin. Cerrina Well #1-32. After Goodman and Malin (1992).

diagram while stratigraphic markers were used to create the models for this project. This might also explain why the 2 Ma loading event shown on the geohistory model created for this project (Figure 16) is not shown on Goodman and Malin's (1992) (Figure 17). Biostratigraphic data might not have been as well preserved in the sediments of the basin due to the fact that the basin was no longer under subaqueous conditions by Late Pliocene time. This would result in a more generalized curve during this time in Goodman and Malin's (1992) model.

Well # 72-4 Geohistory Model

Well #72-4 is located in the Paloma oil field in the center of the study area. The geohistory model for this well is shown in Figure 18. This well is deeper than the Cerrina #1-32 well and penetrates more of the stratigraphic section. It therefore represents a larger segment of time than the Cerrina #1-32 well.

The geohistory model shows relatively steady basin subsidence from 24-15 Ma due primarily to tectonic influences. This can be seen as the blue curve, which represents subsidence due to tectonism, plots alongside the lower black curve, which represents total subsidence (from both tectonism and sediment loading). A period of uplift followed by a brief episode of rapid subsidence occurred from 15-11 Ma as the paleobathymetry within the basin began to decrease at the same time. Uplift and a rapid decrease in paleobathymetry occurred from 11- 9.5 Ma. An episode of subsidence occurred from 9.5 Ma to the present as sediment loading increasingly became the principle mechanism for subsidence in the Pleistocene.

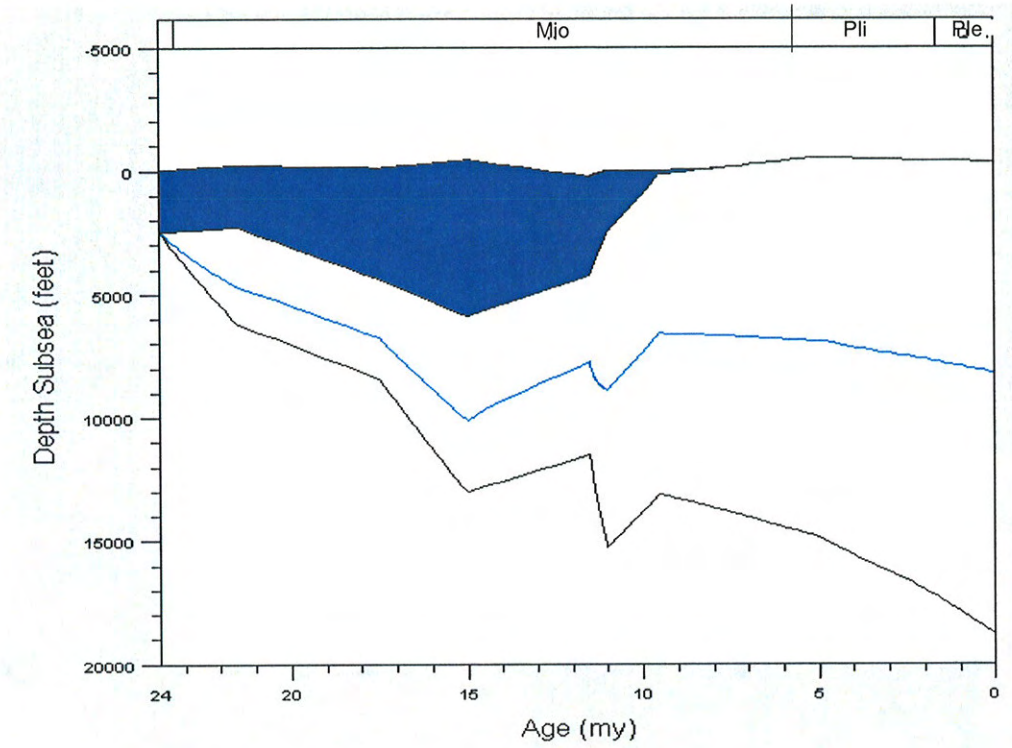

Figure 18. Geohistory model for well #72-4 in the Paloma oil field, central Maricopa sub-basin. Blue shaded area represents paleobathymetry and paleo sea level. The middle curve represents subsidence due to tectonism and the bottom curve represents total subsidence due to tectonism as well as sediment loading. The horizon tracked is the deepest horizon this well penetrates which is the Santos Formation of early Miocene age. Mio=Miocene; Pli=Pliocene; Ple=Pleistocene H=Holocene. Note the increase in subsidence due to sediment loading as age decreases.

Well # 987-25R Geohistory Model

Well # 987-25R is located in the Elk Hills oil field and was used to analyze the subsidence history for the northwest region of the study area. This well is deeper than the Cerrina #1-32 well and penetrates to the Miocene Santos Formation. The geohistory model represents basin history from 24 Ma to the present and is shown in Figure 19.

The geohistory model shows subsidence occurred from 24-15 Ma due primarily to tectonism. This is shown on the geohistory model by the blue curve (subsidence due to

tectonism) plotting parallel to the black curve (total subsidence). This episode of subsidence is similar to that observed in the geohistory model for well #72-4 during the same time period (Figure 18). During this subsidence episode, the Santos Formation reached its maximum depth of ~17,000 feet at ~15 Ma.

The geohistory model shows the region underwent an episode of uplift from 15-9.5 Ma followed by an episode of subsidence from 9.5 Ma to 2 Ma. During this episode of subsidence, the geohistory model shows the total subsidence and tectonic subsidence curves diverge slightly from 5-2 Ma suggesting sediment loading as an increasing factor for subsidence. This latest episode of subsidence was not as pronounced as that shown by the geohistory models for the Cerrina #1-32 and #72-4 wells. The episode of uplift that occured at 2 Ma and continues through the Holocene is not seen in the other two geohistory models for the region.

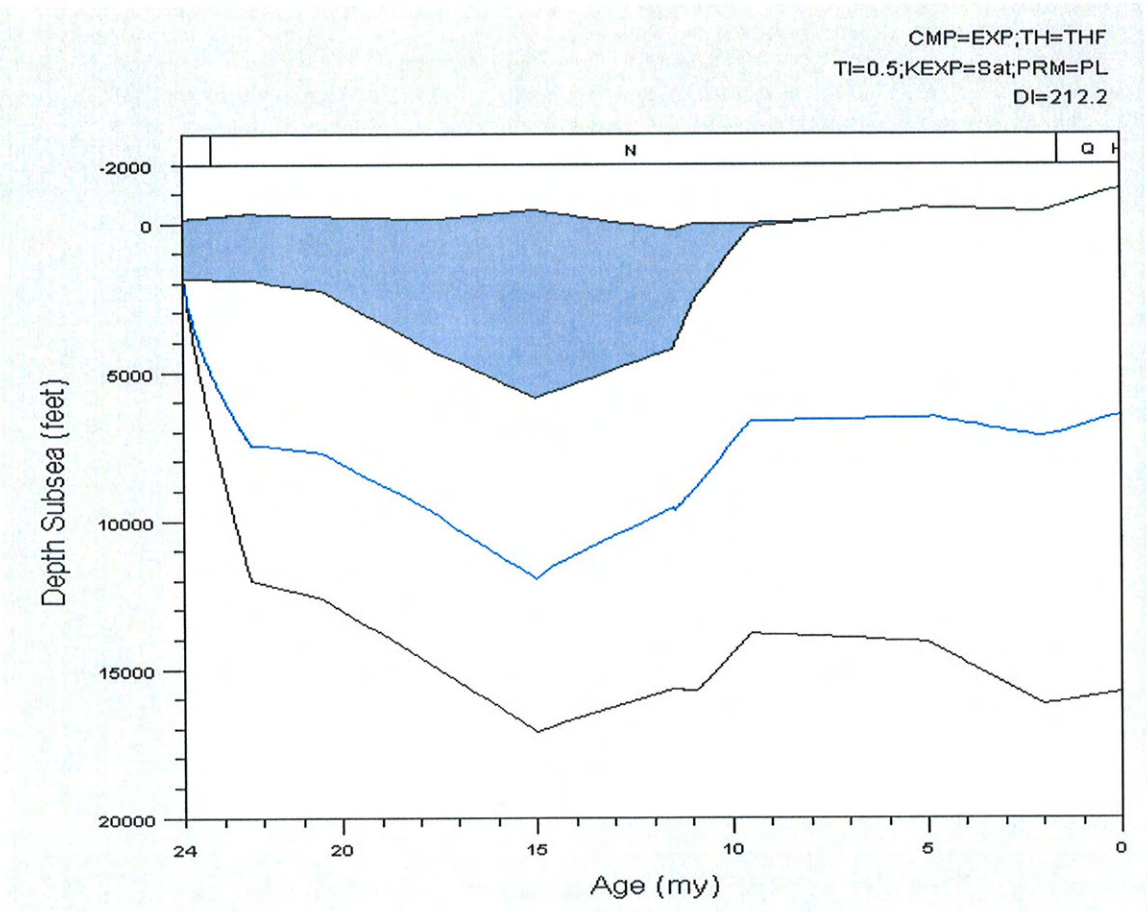

Figure 19. Geohistory model for well #987-25R in the Elk Hills oil field, western Maricopa sub-basin. Blue shaded area represent paleobathymetry and paleo sea level. The middle curve represents subsidence due to tectonism and the bottom curve represents total subsidence due to tectonism as well as sediment loading. The horizon tracked is the deepest horizon this well penetrates which is the Santos Formation of early Miocene age. N=Neogene; Q=Quaternary and H=Holocene. Note the maximum depth at ~15 Ma.

Discussion of Maricopa Sub-basin Models

Regional tectonic events caused subsidence to occur in all areas of the Maricopa sub-basin. The geohistory models suggest subsidence occurred from ~24 Ma to ~15 Ma in the central (#72-4) and from 20 Ma to 15 Ma in the western (#987-25R) Maricopa sub-basin. During Early Miocene time (24-15 Ma), the North American-Pacific plate boundary began a transition from a convergent to a transform plate boundary (Dickinson, 1987). This resulted in the development of right-slip motion along the San Andreas fault. The Mendocino triple junction was located directly to the south of the San Joaquin basin (Bent, 1988) and a convergent plate boundary existed along the basin's west side. The unstable configuration of the migrating triple junction induced an episode of extensional tectonism in nearby regions (Dickinson and Snyder, 1970, Ingersoll, 1982). This regional extensional stress pattern resulted in normal faulting from Late Oligocene to Early Miocene time (Bartow, 1992).

The Mendocino triple junction was directly to the west of the San Joaquin basin at ~15 Ma (Bent, 1988). All three geohistory models show that a change in basin development occurred at this time. The geohistory model for the eastern Maricopa sub-basin shows subsidence took place from 15-12 Ma while the geohistory models for the central and western Maricopa sub-basin show uplift during this same time period. During this time the San Andreas fault continued to develop along the western margin of the San Joaquin basin as the Mendocino triple junction migrated northward. The regional stress pattern changed for the southern region of the San Joaquin basin and was characterized by compression normal to the San Andreas fault (Bartow, 1992). This induced wrench tectonics in conjunction with deep-seated thrusting along the southwest side of the basin adjacent to the San Andreas fault (Bartow, 1992). The earliest conclusive evidence

suggests en echelon folding began along the southwestern margin of the basin at ~16 Ma (Harding, 1976) and may have been the cause of the uplift that began at 15 Ma in the western and central regions of the sub-basin. The subsidence that occurred in the eastern Maricopa sub-basin from 15-12 Ma could be due to the fact that the eastern Maricopa sub-basin is at a greater distance from the San Andreas fault and thus the compressional stress regime may not have had as great an effect on this region of the sub-basin.

The eastern (Cerrina #1-32 well) Maricopa sub-basin experienced uplift from 12-11 Ma while the central (72-4 well) and western (987-25R well) sub-basin experienced subsidence during the same time. By 12 Ma, the Mendocino triple junction had migrated northward past the southern San Joaquin basin and the North American plate underwent thermal thinning of the lithosphere (Crough and Thompson, 1977; Mavko and Thompson, 1983). This may have caused the subsidence that occurred in the western and central regions of the sub-basin. The period of uplift shown on the geohistory model starting at 12 Ma is not apparent on any isochore map because the isochore maps do not represent that period of time. However, this episode of uplift is represented in the stratigraphic record as an unconformity that occurs at the base of the Reef Ridge Formation and its equivalents in the southern region of the study area (Bartow, 1992).

The eastern Maricopa sub-basin also may have been affected by the last major uplift of the Sierra Nevada (Crough and Thompson, 1977; Mavko and Thompson, 1983). This uplift to the east may have resulted in the episode of uplift that occurred at ~12 Ma in the Cerrina #1-32 well. The White Wolf fault (Figure 1) also began to play a major role in basin development in the southern region of the basin (Davis and Lagoe, 1988).

This large, basin-edge, normal fault contributed to subsidence in the southern San Joaquin basin during Middle Miocene to Early Pliocene time (Davis and Lagoe, 1988).

An increase in relative plate motion between the North American and Pacific plates occurred at ~10 Ma (Atwater and Molnar, 1973). Acceleration of the slip rates on the San Andreas fault in latest Miocene time correlated with an increase in deformation in the fold belt adjacent to the fault (Harding, 1976). This acceleration may have contributed to the rapid subsidence in the southern San Joaquin basin (Dickinson and Snyder, 1979; Davis, 1983) and can be seen as the subsidence that occurred in all the geohistory analyses for the sub-basin after 10 Ma. The eastern (#1-32), central (#72-4), and western (#987-25R) geohistory models show subsidence occurred from ~10 Ma through the Pleistocene and that sediment loading was an increasing factor in basin subsidence.

The isochore maps indicate areas of sediment deposition and non-deposition or erosion from 10-0 Ma. The Reef Ridge isochore map represents the accumulation of sediments from ~9-6 Ma. This Late Miocene episode of subsidence (9.5-2 Ma) can be seen in the isochore map of the Reef Ridge Formation (Figure 10) as a slight thickening of sediments between well #987-25R and well #72-4.

Faulting began in the Basin and Range province to the east of the Sierra Nevada in Late Miocene time (~10 Ma) (Zoback et al, 1981). This extensional faulting as well as related left-lateral movement on the Garlock fault is assumed to have begun at about the same time. The result was westward movement of the Sierra Nevada block as well as the San Joaquin basin and, consequently, the formation of a constraining bend along the San Andreas fault at the southern margin of the basin (Bartow, 1992). The space problem

arising from the westward movement probably caused compression normal to the San Andrea fault at the west side of the Sierran block (Wentworth and Zoback, 1986).

At ~5 Ma, the motion of the Pacific plate changed to a more northerly direction, resulting in a component of compression normal to the San Andreas transform (Minster and Jordan, 1984; Page and Engebretson, 1984; Cox and Engebretson, 1983). This compression probably caused uplift of the Temblor and Diablo Ranges and, together with the developing bend in the San Andreas fault, was probably the principle factor leading to northward-directed thrusting at the south end of the basin (Bartow, 1992). The present day San Emigdio Mountains, located at the southern edge of the basin, were folded and uplifted by this system of north vergent thrust faults (Davis and Lagoe, 1988; Davis, 1983). Thrust loading from this event caused flexural subsidence to occur in the southern part of the basin in the latest Pliocene (Bartow, 1992) and is illustrated in the geohistory model of the eastern Maricopa sub-basin as an increase in subsidence at 2 Ma. The concave down shape of the subsidence curve representing the Late Miocene to Pleistocene also suggests subsidence due to thrust loading (Bent, 1988). The isochore map of the Tulare Formation, which represents this segment of time, shows a thickening of sediment in the southeastern Maricopa sub-basin suggesting subsidence occurred at this time.

The geohistory model for the western (#987-25R) Maricopa sub-basin shows a smaller degree of subsidence during Late Miocene to Pliocene time relative to the geohistory models for the central and eastern Maricopa sub-basin. During much of the Pliocene massive amounts of clastic sediments derived from the uplift of the Temblor Range to the west were deposited in the Elk Hills area (Reid, 1991). This caused

subsidence due to sediment loading during the Pliocene (~5-2 Ma). The subsidence can be seen on the isopach maps for the Etchegoin and San Joaquin Formations. Each shows an accumulation of sediments, in the vicinity of well #987-25R.

The difference in basin development in the western Maricopa sub-basin could be due to changes in the regional tectonics through the Pleistocene. Anticlinal growth of the Elk Hills structure along the western edge of the basin began in Late Miocene time due to the compressional stress regime (Reid, 1991). This can be seen in the isochore maps as the region around Elk Hills shows a smaller amount of sediment deposition relative to other regions in the sub-basin. The subsidence at Elk Hills is not as extreme as subsidence in the other geohistory models because Elk Hills lies within a structurally complex, en echelon fold-thrust belt that has developed since Early Miocene time (Davis and Lagoe, 1988). Within this belt, which extends from the Temblor Range 20 to 30 miles eastward into the San Joaquin Valley, en-echelon anticlines and thrust faults grew basinward due to wrench faulting and thrusting (Nicholson, 1990). The geohistory model for the western (#987-25R) Maricopa sub-basin reflects the effects of this structural deformation. The geohistory models for the eastern (Cerrina #1-32) and central (#72-4) Maricopa sub-basin do not lie within the fold-thrust belt and were not as strongly affected by the wrench tectonics to the west. Uplift during the Pleistocene is also indicated in the isochore map of the Tulare Formation (Figure 13) by a thinning of the sediments in the vicinity of well #987-25R.

Discussion of Other Geohistory Analyses in the San Joaquin Basin

Tejon Embayment

Goodman and Malin's (1992) geohistory model for the Tejon embayment (Figure 20) suggests that several kilometers of subsidence of the southernmost San Joaquin basin floor occurred during Late Oligocene and Early Miocene time (~30-12 Ma). They interpreted this subsidence event to be related to regional extension beginning in the Late Oligocene. Their model for the Tejon embayment shows maximum basin subsidence occurred at ~20 Ma followed by overall episodic uplift to 10 Ma. Their model also suggests subsidence occurred in the Late Miocene due to a strong tectonic component. Sediment loading becomes more of an influence on subsidence starting at ~2 Ma.

Goodman and Malin's (1992) model differs from the models created for this study in that the models created for this study begin with Early Miocene time whereas Goodman and Malin's model extends back to Oligocene time. In the geohistory models created for this study (Figures 16, 18, and 19), the Maricopa sub-basin subsided from 20 Ma to ~ 15-12 Ma (Early to Middle Miocene time) which is later than suggested in the Goodman and Malin (1992) study.

For Pliocene to Pleistocene time the model for the Tejon embayment and the models for the central and eastern Maricopa sub-basin show a concave-down shape as they illustrate subsidence continuing to present day. This is typical of the shape of subsidence history curves from foreland basins (Dickinson, 1979). For this time period, the Maricopa and Tejon sub-basins underwent subsidence due increasingly to sediment loading as opposed to earlier in their histories where subsidence was due principally to tectonism. The Tejon embayment geohistory model suggests more of an influence by tectonic loading than is shown in the geohistory model for the Maricopa sub-basin early

in the Pliocene. The geohistory model for the western Maricopa sub-basin shows uplift occurring at present day, which is not consistent with the total subsidence curve on the geohistory model of the Tejon embayment.

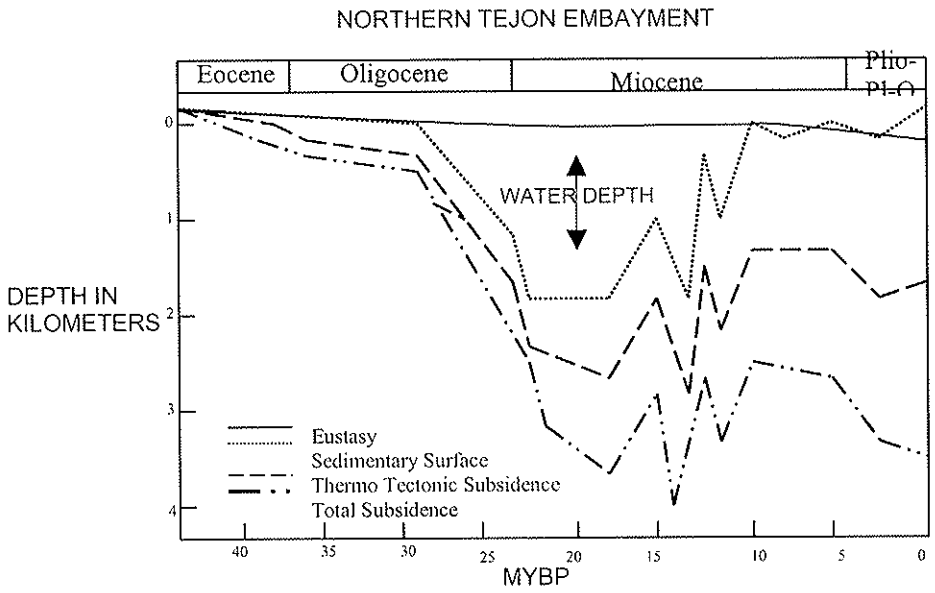

Figure 20. Tejon embayment geohistory model after Goodman and Malin (1992). This geohistory diagram is taken from a well to the south of this projects Cerrina 1-32 well in T11N R20W. Note the episode of initial subsidence occurs earlier in the history of the Tejon Embayment (~30Ma) relative to the Maricopa sub-basin.

Lost Hills

Rentschler and Bloch's (1988) geohistory models were constructed based on data from two wells on the western margin of the San Joaquin basin north of the study area: the Texaco 'Beer' #66-7 well and the American Quasar 'Bravo' #31-1 well. Figure 21 shows the location of these two wells within the valley. These wells penetrated more of the stratigraphic section and the geohistory models represent a larger segment of time

than the geohistory models created for the Maricopa sub-basin in this study. The following comparison of the data will begin at ~20Ma because the geohistory models of the Maricopa sub-basin start at this time.

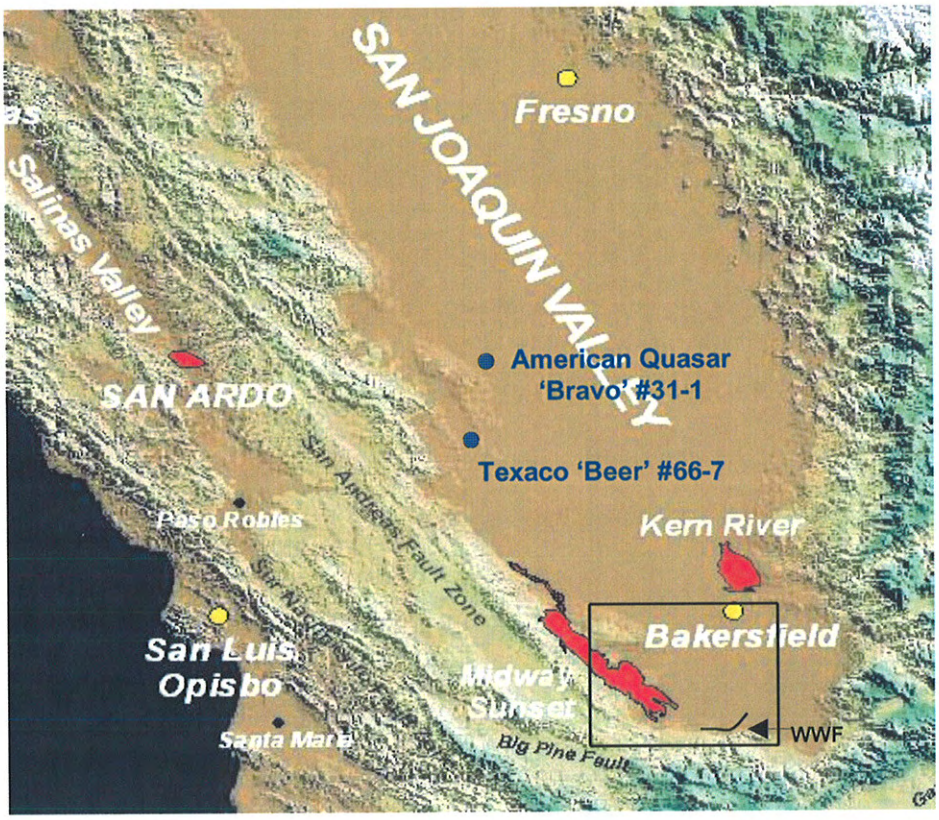

Figure 21. Map showing location of wells used in Rentschler and Bloch's (1988) geohistory models. The black box represents general location of the study area in this report. WWF= White Wolf Fault.

The geohistory models for the 'Beer' and 'Bravo' wells are shown in Figure 22. The curves for the 'Bravo' well have a generally concave down shape while those for the 'Beer' well have an overall concave up shape. From 20 Ma, the geohistory model for the 'Beer' well shows an episode of subsidence followed by an episode of uplift at 9 Ma

possibly caused by tilting of the Sierra Nevada to the east (Rentschler and Bloch, 1988). This uplift began ~9 Ma and persists to the present day. It contrasts with the geohistory model for the eastern and central Maricopa sub-basin which shows uplift ended at ~10 Ma and subsidence occurred thereafter to present day. Also, the maximum subsidence of

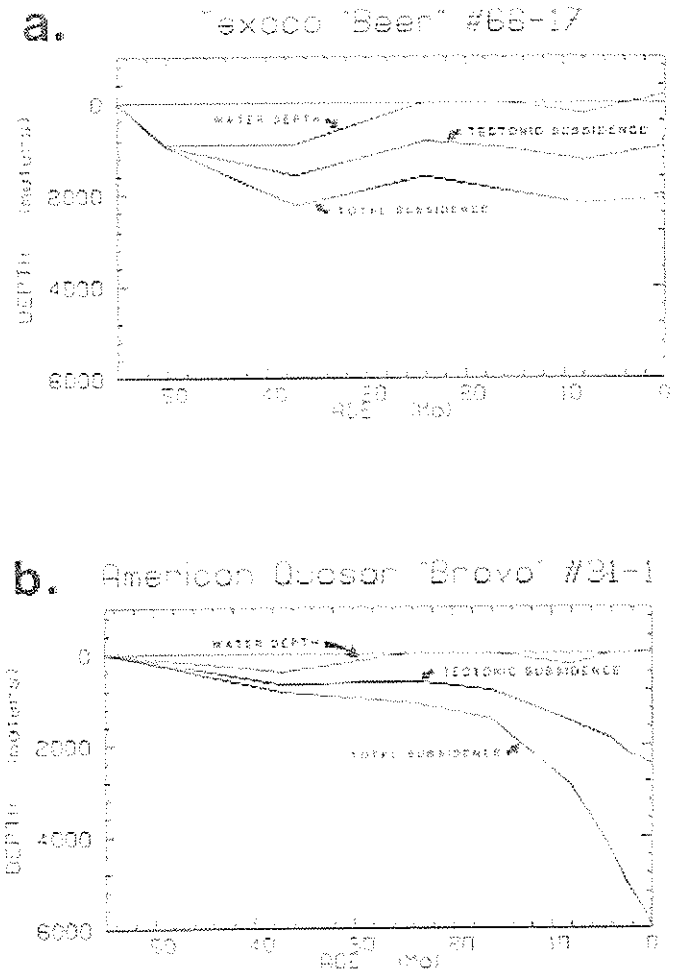

Figures 22. Contrasting Geohistory models of the northern San Joaquin basin (Rentschler and Bloch, 1988). a. is the Texaco 'Beer' #66-17 well which is located to the south of Rentschler and Bloch's project area (see figure 17). b. is the geohistory analysis for the American Quasar 'Bravo' #31-1 well which is located to the northeast of Rentschler and Bloch's project area.

the basin occurred at 9 Ma in the 'Beer' well while the geohistory models for the eastern and central Maricopa sub-basin all show the maximum depth occurring at present day. The shape of the geohistory curves for the 'Beer' well is similar to that of the geohistory model for the western Maricopa sub-basin. Rentschler and Bloch (1988) claimed that subsidence rates in the area represented by the 'Beer' well have been generally decreasing through time. The subsidence rate for the western Maricopa sub-basin has not decreased but has increased to a smaller degree than in the eastern and central areas of the sub-basin.

The model for the 'Bravo' well has a concave down subsidence curve but it does not resemble the overall shape of curves of the Maricopa sub-basin from ~20-10 Ma. The model from the 'Bravo' well shows that the area experienced continuous subsidence during this time period whereas each geohistory model for the Maricopa sub-basin shows uplift occurred sometime during this time period. The geohistory model shows subsidence rates at the location of the 'Bravo' well have increased. The most rapid subsidence occurred in the last 8 Ma (Rentschler and Bloch, 1988). This is similar to the geohistory models for the eastern and central Maricopa sub-basin. The eastern and central Maricopa sub-basin both show an increase in subsidence occurred at ~10 Ma which continues to present day. This increase in subsidence at ~10 Ma gives the geohistory models a concave down shape. A concave down subsidence curve is typical of foreland basins (Dickinson, 1979) and Moxon and Graham (1987) suggest this shape corresponds with thrust loading as the likely mechanism for basin subsidence (Rentschler and Bloch, 1988).

CONCLUSION

The transition between plate tectonic boundaries during the Oligocene and Early Miocene affected the evolution of the Maricopa sub-basin. The geohistory models created in this study illustrate mechanisms for basin evolution from Miocene to Quaternary time and relate them to regional tectonism. The isochore maps created for four stratigraphic units illustrate lateral continuity of thickness trends of individual stratigraphic units within the Maricopa sub-basin. These maps illustrate the extent of local areas of subsidence and uplift within the Maricopa sub-basin.

The geohistory models show the Maricopa sub-basin underwent subsidence in Early to Middle Miocene time (~20-12 Ma). The sub-basin was affected by the regional tectonics of the plate boundary transition from convergent to transform. The Mendocino triple junction migrated northward past the west side of the basin during the Miocene epoch. Adjacent to the developing San Andreas system, east-west oriented normal faulting and subsidence began in the latest Oligocene and Early Miocene indicating north-south extension (Bartow, 1992). High-angle faults of Late Oligocene to Early Miocene age represent the initiation of this phase of subsidence in the basin (Davis and Lagoe, 1988).

The geohistory models suggest the Maricopa sub-basin underwent uplift in Middle Miocene time. Uplift of the southern portion of the San Joaquin basin occurred in Middle Miocene time (~15Ma) and coincided with a eustatic marine regression (Bartow, 1992). The initiation of wrench tectonism on the southwest side of the Maricopa sub-basin resulted in uplift along the edge of the basin.

At the end of the Miocene, the geohistory models suggest a return to subsidence throughout the basin that continues to present day in the central and eastern regions of the Maricopa sub-basin. This Late Miocene to Early Pliocene subsidence was partially controlled by normal fault movement along the White Wolf fault (Davis and Lagoe, 1988). This structural style is different than the earlier phase of extensional faulting in Early Miocene time. The Early Miocene phase of subsidence occurred along listric-shaped normal faults. The absence of listric-shaped extensional faults during this later period of basin development suggests that Middle Miocene to Pliocene subsidence is not entirely the result of extension and that other mechanisms may be operating to contribute to subsidence (Davis and Lagoe, 1988).

Late Pliocene to Quaternary thrusting along the southern edge of the basin caused uplift of the San Emigdio Mountains and Transverse Ranges to the south and subsidence of the basin directly to the north (Namson and Davis, 1988; Davis and Lagoe, 1988). This thrusting coincided with a period of increased convergence between the North American and Pacific plates (Cox and Engebretson, 1983) and the development of a constraining bend in the San Andreas fault due to Basin and Range spreading to the east. Subsidence episodes from Late Miocene time to the present differed in magnitude depending on the location in the sub-basin. The eastern and central geohistory models of the Maricopa sub-basin show that subsidence occurred during the Late Pliocene to Quaternary time. The geohistory model of the 987-25R well in the western region of the sub-basin shows a lesser magnitude of subsidence relative to the geohistory models for wells to the east. This episode of uplift is not seen in the other two geohistory models to

the southeast and may be due to wrench tectonics along the San Andrea fault caused by a compressional stress regime.

The geohistory models for the Maricopa sub-basin are both similar and different from other geohistory models in the San Joaquin basin primarily as a consequence of the proximity of the study area to the plate boundary and varying tectonic histories. The Tejon embayment geohistory model suggests that the major subsidence and uplift events were controlled by tectonics from the Late Oligocene to the Early Miocene. This changed as the magnitude of tectonic fluctuations decreased from Late Miocene time implying sediment loading was an increasing factor in basin subsidence. This is similar to the geohistory models for the central and eastern Maricopa sub-basin.

Goodman and Malin's (1992) geohistory model for the Tejon embayment also differs from the geohistory models created for this study. The Tejon embayment model shows maximum subsidence occurred earlier (~12 Ma) while the models for the eastern and central Maricopa sub-basin show maximum subsidence at present day. Basin development for the Tejon embayment was due to episodes of Oligocene/Miocene normal faulting and, in Pliocene to recent time, primarily due to loading of thrust sheets and high rates of sedimentation. The Maricopa sub-basin subsidence is greater in magnitude at present day and is due primarily to sediment loading.

Rentschler and Bloch's (1988) two geohistory models for the Lost Hills area of the San Joaquin basin are somewhat similar in shape to the geohistory models of the Maricopa sub-basin with some differences. The 'Beer' well geohistory model shows the maximum magnitude of subsidence occurred at 9 Ma whereas the Maricopa sub-basin models presented here show maximum magnitude of subsidence of the central and

eastern regions of the sub-basin occurring at present day. From ~10 Ma to present the geohistory models of the 'Bravo' well and those created for the Maricopa sub-basin are similar in shape. Both exhibit an overall concave downward geometry indicating thrust or sediment loading as the mechanism for subsidence, which is typical of a foreland basin setting (Bent, 1988).

REFERENCES

Addicott, W.O., 1968, Mid Tertiary zoogeographic and paleogeographic discontinuities across the San Andreas fault, *in* Dickinson, W.R., and Grantz, A., eds., Proceeding of Conference on Geologic Problems of the San Andreas Fault System: Stanford University Publications, Geologic Sciences, v. 11, p. 144-165.

Atwater, T., 1970, Implications of Plate Tectonics for the Cenozoic Tectonic Evolution of Western North America: Geological Society of America, v. 81, p. 3513-3536.

Atwater, T., and Molnar, P., 1973, Relative motion of the Pacific and North American plates deduced from sea-floor spreading in the Atlantic, Indian, and South Pacific Oceans, *in* Kovach, R.L., and Nur, A., eds., Proceedings of Conference on the Tectonic Problems of San Andreas Fault System: Stanford University Publication, Geological Sciences, v. 13, p. 136-148.

Bandy, O.L., and Arnal, R.E., 1969, Middle Tertiary basin development, San Joaquin Valley, California: Geological Society of America, v. 80, p. 783.

Barbat, W.F., and Johnson, F.L., 1934, Stratigraphy and Foraminifera of the Reef Ridge Shale, Upper Miocene, California: Journal of Paleontology, v. 8, p. 3-17.

Bartow, A.J., 1991, The Cenozoic Evolution of the San Joaquin Valley, California: U.S Geological Survey Professional Paper 1501, 40 p.

Bartow, A.J., 1992, Cenozoic stratigraphy of the northern San Joaquin Valley, Central California, *in* Erksine, M.C., Unruh, J., and Lettis, W.R., eds., Field Guide to the Tectonics of the Boundary Between the Coast Ranges and the Great Valley of California, GB-70, 5 p.

Bent, J.V., 1988, Paleotectonics and provenance of Tertiary sandstones of the San Joaquin basin, California, *in* Graham, Stephan A., ed., Studies of the geology of the San Joaquin Basin: Pacific Section S.E.P.M., v. 60, p. 65-87.

Critelli, S., and T.H. Nilsen, 2000, Provenance and stratigraphy of the Eocene Tejon Formation, western Tehachapi Mountains, San Emigdio Mountains and Southern San Joaquin Basin, California: Sedimentary Geology, v. 136, p. 7-27.

Clarke, S.H., Howell, D.G., Nilsen, T.H., 1975, Paleogene geography of California *in* Weaver, D.W., Hornday, G.R., and Tipton, A., eds., Paleogene symposium and selected technical papers: American Association of Petroleum Geologists-Society of Economic Paleontologists and Mineralogists-Society of Exploration Geophysicists, Pacific Section, Annual Meeting, 1975, p. 121-154.

Cox, A., and Engebretson, D.C., 1983, Change in motion of Pacific plate at 5 Ma.: Nature, v. 313, p. 472-474.

Crough, S.T., and Thompson, G.A., 1977, Upper mantle origin of the Sierra Nevada uplift: Geology, v. 5, p. 396-399.

Davis, T.L., 1983, Late Cenozoic structure and tectonic history of the western "Big Bend" of the San Andreas fault and adjacent San Emigdio Mountains: University of California, Santa Barbara Ph.D. Thesis, 580 p.

Davis, T.L., and Lagoe, M.B., 1988, A structural interpretation of major tectonic events affecting the western margins of the San Joaquin Valley, California, *in* Graham, Stephan A., ed., 1988, Studies of the geology of the San Joaquin Basin: Pacific Section S.E.P.M., Vol. 60, p.65-87.

DeCelles, P.G., 1988, Middle Cenozoic depositional, tectonic, and sea level history of the Southern San Joaquin Basin, California: American Association of Petroleum Geologists Bulletin, v. 72, p. 1,297.

Dibblee, T.W. Jr., 1971, Geologic maps of fourteen 15-minute quadrangles along the San Andreas fault in the vicinity of Paso Robles and Cholame southeastward to Maricopa and Cuyama: U.S. Geological Survey open File Map 71-87, scale 1:62,500.

Dibblee, T.W. Jr., 1973, Regional geologic map of San Andreas and related faults in Carrizo Plain, Temblor, Caliente, and La Panza Ranges and vicinity, California: U.S. Geological Survey Map I-757, scale 1:125,000.

Dibblee, T.W. Jr., 1974, Geologic map of the Shandon and Orchard Peak quadrangles, San Luis Obispo and Kern counties, California: U.S. Geological Survey Map I-788, scale 1:62,000.

Dickinson, W.R., 1979, Plate tectonic evolution of sedimentary basins *in* Plate Tectonics and Hydrocarbon Accumulation, American Association of Petroleum Geologists Continuing Education Course Notes, p. 1-62.

Dickinson, W.R., Armin, R.A., Beckvar, N., Goodlin, T.C., Janecke, S.U., Mark. R.A., Norris, R.D., Radel, G., and Wortman, A.A., 1987, Geohistory analysis of rates of sediment accumulation and subsidence for selected California basins, *in* Ingersoll, R.V., and Ernst, W.G., eds., Cenozoic Basin Development of Coastal California, Prentice Hall Inc, New Jersey, p. 1-23.

Dickinson, W.R., 1987, Plate tectonics and the continental margin of California, *in* Ernst, W. G., ed., The Geotectonic Development of California, Prentice Hall New Jersey p. 2-28.

Dickinson, W.R., and Snyder, W.S., 1979, Geometry of triple junctions related to San Andreas transform: Journal of Geophysical Research, v. 84, p. 561-572.

Engebretson, D.C., Cox, A., and Gordon, R.G., 1985, Relative motions between oceanic and continental plates in the Pacific basin: Geological Society of America Special Paper 206, 59 p.

Erskine, M.C., 1992, Interpretive structural cross section from the central Diablo Range to the San Joaquin Valley, California, *in* Erskine, M.C., Unruh, J., and Lettis, W.R., eds., Field Guide to the Tectonics of the Boundary Between the Coast Ranges and the Great Valley of California GB-70, p. 23.

Fedewa, W.T., and Simmons, M.L., 1997, Depositional model for the potter sand member of the Reef Ridge formation, Midway Sunset field, kern County, California: American Association of Petroleum Geologist Bulletin, v. 81, p. 685.

Goodman, E.D., 1989, The Tectonics of Transition Along an Evolving Plate Margin-Cenozoic Evolution of the Southern San Joaquin Basin, California: University of California, Santa Barbara, Ph. D. Thesis, 208 p.

Goodman, E.D., and Malin, P.E., 1992, Evolution of the southern San Joaquin Basin and the Mid–Tertiary "Transitional" Tectonics, Central California: *Tectonics*, v. 11, p. 478-498.

Gorsline, D.S., and Douglas, R.G., 1987, Analysis of sedimentary systems in active margin basins: California Continental Borderland, *in* Ingersoll, R.V., and Ernst W.G., eds., Cenozoic Basin Development of Coastal California, p. 64-80.

Graham, S.A., 1978, Role of Salinian block in evolution of San Andreas fault system: American Association of Petroleum Geologists Bulletin, v. 62, p. 2214-2231.

Graham, S.A., 1987, Tectonic controls on petroleum occurrence in central California, *in* Ingersoll, R.V., and Ernst W.G., eds., Cenozoic Basin Development of Coastal California, p. 47-63.

Graham, S.A., and Berry, K.D., 1979, Early Eocene Paleogeography of the central San Joaquin Valley: Origin of the Cantua Sandstone, *in* Armentrout, J.M., Cole, M.R., and TerBest, H.Jr., eds., Cenozoic Paleogeography of the Western United States: Society of Economic and Paleontologists and Mineralogists, Pacific Section Annual Meeting Aneheim, CA., p. 119-127.

Graham, S.A, Williams, L.A., Bate, M., and Weber, L.S., 1982, Stratigraphic and depositional framework of the Monterey Formation and associated coarse clastics of the central San Joaquin basin, *in* Williams, L.A. and Graham, S.A., eds., Monterey Formation and associated coarse clastic rocks, central San Joaquin basin, California: Pacific Section SEPM, Annual Field Trip Guidebook, p. 3-16.

Graham, S.A., and Williams, L.A., 1985, Tectonic, depositional and diagenetic history of Monterey Formation (Miocene), central San Joaquin basin, California: American Association of Petroleum Geologists Bulletin, v. 69, p. 385-411.

Greene, H.G., and Clarke, J.C., 1979, Neogene paleogeography of the Monterey Bay area, California, *in* Armentrout, J.M., Cole, M.R., and TerBerst, H. Jr., eds., Cenozoic paleogeography of the western United States: Society of Economic Paleontologists and Mineralogists, Pacific Sections, Annual Meeting, Anaheim California, Pacific Coast Paleogeography Symposium 3, p. 217-238.

Harding, T.P., 1976, Tectonic significance and hydrocarbon trapping consequences if sequential folding synchronous with San Andreas faulting, San Joaquin Valley, California: American Association of Petroleum Geologists Bulletin, v. 60, p. 356-378.

Hardoin, J.L., 1962, North Coles Levee Oil Field, *in* Summary of Operations California Oil Field: Division of Oil and Gas, v. 48, p. 53-63.

Haq, B.U., Hardenbol, J., and Vail, P.R., 1987, Chronology of fluctuating sea levels since the Triassic: Science v. 32, p. 1156-1167.

Huffman, O.F., 1972, Lateral displacement of upper Miocene rocks and the Neogene history of offset along the Sam Andreas fault in central California: Geological Society of America Bulletin, v.83, p. 2913-2946.

Ingersoll, R.V., 1978, Paleogeography and paleotectonics of the late Mesozoic forearc basin of northern and central California, *in* Howell, D.G., and McDougall, K.A., Mesozoic Paleogeography of the western United States: Pacific Section, Society of Economic Paleontologists and Mineralogists Paleogeography Symposium 2, p. 471-482.

Ingersoll, R.V., 1979, Evolution of the late Cretaceous forearc basin, northern and central California: Geological Society of America Bulletin, v. 90, p. 813-826.

Ingersoll, R.V., 1982, Initiation and evolution of the Great Valley forearc basin of northern and central California: American Association of Petroleum Geologists Bulletin, v. 67, p. 1125-1142.

Ingersoll, R.V., 1988, Development of the Cretaceous forearc basin of central California, *in* Graham, S.A. ed., Studies of the Geology of the San Joaquin Basin: Pacific Section S.E.P.M., v. 60, p. 141-155.

Jones, C.L., and Gillespie, J.M., 1997, Listric normal faults in the Miocene-Pliocene section at north and south Coles Levee fields: A response to Pleistocene growth of the Elk Hills anticline, *in* Girty, G.H., Hanson, R.E., and Cooper, J.D., eds., Geology of the Western Cordillera: Perspectives from Undergraduate Research: Pacific Section Society of Economic Paleontologists and Mineralogists, v. 82, p. 49-56.

Link, M.H., Helmold, K.P., Long, W.T., 1990, Depositional environments and reservoir characterization of the upper Miocene Etchegoin and Chanac Formations, Kern Front Oil Field, California, *in* Kuespert, J.G., and Ried, S.A., eds., Structure, Stratigraphy and Hydrocarbon Occurrences of the San Joaquin Basin, California: Society of Economic Paleontologist and Mineralogists, p. 73-96.

Loomis, K.B., 1990, Depositional environments and sedimentary history of the Etchegoin Group, west-central San Joaquin Valley, California, *in* Kuespert, J.G., and Ried, S.A., eds., Structure, Stratigraphy and Hydrocarbon Occurrences of the San Joaquin Basin, California: Society of Economic Paleontologist and Mineralogists, p. 231-246.

MacPherson, B.A., 1978, Sedimentation and trapping mechanism in upper Miocene Stevens and older turbidite fans of southeastern San Joaquin Valley, California: American Association of Petroleum Geologist Bulletin, v. 62, p. 2243-2278.

Maher, J.C., Carter, R.C., and Lantz, R.J., 1975, Petroleum geology of naval petroleum reserve No.1 Elk Hills, Kern County, California: U.S. Geological Society Professional Paper 912, 109 p.

Mavko, B.B., and Thompson, G.A., 1983, Crustal and upper mantle structure of the northern and central Sierra Nevada: Journal of Geophysical Research, v. 88, p. 5874-5892.

McPherson, J.G., and Miller, D.D., 1990, Depositional Setting and reservoir characteristics of the Plio-Pliestocene Tulare formation, South Belridge Field, San Joaquin Valley, California, *in* Kuespert, J.G., and Ried, S.A., eds., Structure, Stratigraphy and Hydrocarbon Occurrences of the San Joaquin Basin, California: Society of Economic Paleontologist and Mineralogists, p. 205-214.

Minster, J.B., and Jordan, T.H., 1984, Vector constraints on Quaternary deformation on the western United States east and west of the San Andreas fault, *in* Crouch, J.K., and Bachman, S.B., eds., Tectonics and sedimentation along the California margin: Society of Economic Paleontologists and Mineralogists, Pacific Section, Annual Meeting, 1984, p. 1-16.

Moxon, I.W., 1986, Subsidence history of the San Joaquin-Sacramento Valleys: Forearc evolution coupled to convergent margin tectonics: International Sedimentological Congress, 12th, p. 220.

Moxon, I.W., and Graham, S.A., 1987, History and controls of subsidence in the Late Cretaceous-Tertiary Great Valley forearc basin, California: Geology, v. 15, p. 626-629.

Namson, J.S., and Davis, T.L., 1988, Seismically active fold and thrust belt the San Joaquin Valley, central California: Geological Society of America Bulletin, v. 100, p.257-273.

Nicholson, G.E., 1990, Structural Overview of Elk Hills, *in* Kuespert, J.G., and Ried, S.A., eds., Structure, Stratigraphy and Hydrocarbon Occurrences of the San Joaquin Basin, California: Society of Economic Paleontologist and Mineralogists, p. 133-140.

Nilsen, T.H., 1972, Stratigraphy and sedimentation of the Tejon Formation, San Emigdio Mountains, California: Pacific Petroleum Geologist Newsletter, Pacific Section, American Association of Petroleum Geologists, v. 26, p. 5.

Nilsen, T.H., 1979, Early Cenozoic stratigraphy, tectonics and sedimentation of the central Diablo Range between Hollister and New Idria, *in* Nilsen, T.H., and Dibblee, J.W., Jr., eds., Geology of the central Diablo Range between Holloster and New Idria, California: Geological Society of America, Cordilleran Section, Field Trip Guidebook, p. 607.

Nilsen, T.H., 1984, Oligocene tectonics and Sedimentation, California: Sedimentary Geology, v. 37, p. 305-336.

Nilsen, T.H., 1987, Paleogene tectonics and sedimentation of coastal California, *in* Ingersoll, R.V., and Ernst W.G., eds., Cenozoic Basin Development of Coastal California, p. 81-132.

Nilsen, T.H., and Dibblee, T.W. Jr., and Addicott, W.O., 1973, Lower and Middle Tertiary Stratigraphic Units of the San Emigdio and Western Tehachapi Mountains, California: Geologic Survey Bulletin 1372-H, 23 p.

Nilsen, T.H., and Link, M.H., 1975, Stratigraphy, sedimentology and offset along the San Andreas fault of Eocene to lower Miocene strata of the northern Santa Lucia Range and the San Emigdio Mountains, Coast Ranges, central California, *in* Weaver, D.W., Hornaday, G.R., and Tipton, A., eds., Future Energy Horizons of the Pacific Coast, Annual Meeting, Pacific Sections, American Association of Petroleum Geologists, S.E.P.M., S.E.G., p. 367-400.

Nilsen, T.H., and McKee, E.H., 1979, Paleogene paleogeography of the western United States, *in* Armentrout, J.M., Cole, M.R., and TerBerst, H. Jr., eds., Cenozoic paleogeography of the western United States: Society of Economic Paleontologists and Mineralogists, Pacific Sections, Annual Meeting, Anaheim California, Pacific Coast Paleogeography Symposium 3, p. 257-276.

Olsen, H.C., Miller, G.E., and Bartow, J.A., 1986, Stratigraphy, paleoenvironment and depositional setting of Tertiary sediments, southeastern San Joaquin basin, *in* Structure and Stratigraphy of the east side San Joaquin Valley: American Association of Petroleum Geologists Pacific Section, Southeast San Joaquin Valley Field Trip, Guidebook, p. 18-56.

Page, B.M., and Engebretson, D.C., 1984, Correlation between the geologic record and computed plate motions fro central California: Tectonics, v. 3, p.133-155.

Peirce, G.G., 1949, Paloma Oil Field, *in* Summary of Operations California Oil Field; Division of Oil and Gas, v. 35, p. 5-10.

Pence, J.J., 1985, Sedimentology of the Temblor Formation n the northern Temblor Range, California, *in* Graham, S.A., ed., Geology of the Temblor Formation, western San Joaquin basin, California: Society of Economic, Paleontologists and Mineralogists, Pacific Section, Fall 1985 Field Trip, Coalinga California, Guidebook, p. 19-34.

Reid, S.A., 1991, Influence of anticlinal growth on upper Miocene turbidite deposits, Elk Hills Field, Kern County, California: American Association of Petroleum Geologists Bulletin, v. 75, p. 378.

Reid, S.A., 1995, Miocene and Pliocene depositional systems of the southern San Joaquin basin and formation of sandstone reservoirs in the Elk Hills area, California, *in* Fritsche, E.A., Cenozoic Paleogeography of the Western United States – II: Pacific Section, Society of Economic Paleontologist and Mineralogist, p. 131-151.

Reid, S.A., and McIntyre, J.L., 2001, Monterey Formation pocelanite reservoirs of the Elk Hills field, Kern County, California: American Association of Petroleum Geologists v. 85, p. 169-189.

Rentschler, M.S., and Bloch, R.B., 1988, Flexural subsidence modeling of the Tertiary San Joaquin basin, *in* Graham, S.A., ed., Studies of the Geology of the San Joaquin Basin: Pacific Section S.E.P.M., v. 60, p. 29-52.

Repenning, C.A., 1960, Geologic summary of the Central Valley of California, with reference to the disposal of liquid radioactive waste: US Geological Survey Trace Elements Investigation Report 769, 69 p.

Seigfus, S.S., 1934, Stratigraphic features of Reef Ridge shale in southern California: American Association of Petroleum Geologists, v. 23, p. 23-44.

Slagle, L.P., 1979, Depositional systems and structures of the idle Eocene Domengine-Yokut Sandstone, Vallecitos, California: Stanford California, Stanford University, M.S., thesis, p. 1-59.

Stanley, R.G., 1985, Middle Tertiary sedimentation and tectonics of the La Honda basin, central California: U.S. Geological Survey open File report 85-596, 263 p.

Van Hinte, J.E., 1978, Geohistory Analysis-Application of micropaleontology in exploration geology: American Association of Petroleum Geology Bulletin, v. 62, p. 201-222.

Webb, G.W., 1981, Stevens and earlier Miocene turbidite sandstones, southern San Joaquin Valley, California: American Association of Petroleum Geologists Bulletin, v. 65, p. 438-465.

Wentworth, C.M., and Zoback, M.D., 1986, An integrated faulting model for the Coalinga earthquake: A guide to thrust deformation along the Coast Range-Great Valley boundary: Eos, v. 67, p. 1222.

Zoback, M.L., Anderson, R.E., and Thompson, G.A., 1981, Cenozoic evolution of the state of stress and style of tectonism of the Basin and Range province of the western United States: Philosophical Transaction of the Royal Society of London, Series A, v. 300, p. 407-434.

Appendix

API	Well #	Location	Driller TD (ft)	TOP OF UNIT (Measured depths in feet)				
				Tulare Fm.	San Joaquin Fm.	Etchegoin Fm.	Reef Ridge Fm.	Monterey Fm.
4029057500000	D-3	7 32S 23E	12,514					1,700
4029153780000	78-31	31 32S 23E	11,438					4,100
4029602320000	1-3	33 32S 23E	11,011	12			2,180	3,500
4029373130000	12-28	28 32S 23E	10,411					3,800
4029112050000	25P-10D	10 32S 24E	14,622		1,040	2,870	3,630	4,030
4029174400000	1	1 32S 24E	11,886		1,260	4,630	3,530	9,380
4029648690000	86-24	24 32S 24E	10,005	15	3,230	5,870	7,170	8,800
4029809530000	516X	16 32S 24E	10,042	22	2,300	3,360	4,525	5,010
4030003060000	723	9 32S 24E	11,913			2,280	3,900	6,350
4029012950000	1	28 32S 25E	14,015		2,520	7,010	10,170	10,460
4029212390000	18-3	3 32S 25E	13,103		2,900	5,890	8,200	10,200
4029493670000	1	15 32S 25E	16,500	23	1,670	4,350	8,840	9,685
4029539710000	88	8 32S 25E	13,850		3,670	8,500	9,200	12,000
4029593710000	1	11 32S 25E	12,917		3,660	7,050	8,658	11,030
4029607610000	1-13B-N	13 32S 25E	13,000	20	4,560	7,700	9,900	11,590
4029712160000	373-18H	18 32S 25E	12,868		1,970	4,770	7,960	8,103
4030119330000	67X-30	30 32S 25E	12,509	30	4,700	6,800	8,400	9,120
4030034570000	22-1	22 32S 25E	12,993	28	1,450	7,090	9,710	10,330
4029211810000	1	6 32S 26E	12,700		5,760	10,270	11,470	
4029216440000	83-12	12 32S 26E	10,870	0	3,430	6,920	9,890	10,750
4029217310000	72-4	4 32S 26E	21,482		3,120	5,600	8,710	9,400
4029238520000	81-14	14 32S 26E	11,456		3,570	6,840	9,360	104,000
4029295580000	45-11	11 32S 26E	12,507		3,530	6,100	8,950	10,020
4029355060000	54-9 -or- #1	9 32S 26E	11,467		2,795	6,270	8,790	10,605
4029365960000	11-24	24 32S 26E	13,600		4,170	8,060	11,050	12,250
4029376370000	1	30 32S 26E	13,617	15	5,760	10,270	11,470	13,350
4029601690000	1	21 32S 26E	15,222	25	5,210	9,200	11,720	13,650
4029005260100	1	8 32S 27E	15,305	13	5,475	9,800	11,500	12,050
4029216470000	67-6	6 32S 27E	12,792		5,548	9,648	11,240	12,150
4029324220000	83-17	17 32S 27E	13,521		3,860	7,210	10,310	11,010
4029324230000	71	21 32S 27E	15,414		4,030	8,720	11,260	14,300
4029354770000	41-18	18 32S 27E	12,323		3,208	9,199	10,900	
4029487490000	334-4B	4 31S 23E	10,000	11	770	3,820	6,635	7,850
4029432450000	1-16	16 31S 23E	10,003		2,090	4,100	6,450	7,150
4029430390001	924	20 31S 23E	10,850	12	1,300	2,310	3,950	4,780
4029435810000	32X-26B	26 31S 23E	13,991	13	1,370	2,800	3,740	4,255
4029019110000	552	27 31S 23E	11,212		1,500	2,370	3,590	3,895
4029533800000	9-354-4G	4 31S 24E	18,270	31	700	3,020	4,510	6,230
4029626670000	326-9G	9 31S 24E	11,500	21	7,100	9,450	13,350	14,810
4029654790000	USTAN-POC-	22 31S 24E	13,600			5,890	9,225	11,100
4029174100101	33X-30	30 31S 24E	10,030	12	2,020	3,550	6,150	6,720
4029032760000	13-5M	5 31S 25E	16,246				8,400	8,650
4029769690000	22X-10	10 31S 25E	13,497	20	1,700	4,210	7,170	8,020
4029112970000	65-13	13 31S 25E	11,050		3,140	4,750	9,540	10,000
4029294160000	61.00	14 31S 25E	10,010		2,250	5,400	9,170	9,640
4029455240000	12-20M	20 31S 25E	13,608	12	3,010	6,680	11,105	11,850
4029501700000	1.00	26 31S 25E	16,455	12	2,900	5,950	9,436	10,470
4029739570000	1.00	33 31S 25E	14,500	10	4,110	7,240	9,430	12,050

API	Well #	Location	Driller TD (ft)	TOP OF UNIT (Measured depths in feet)				
				Tulare Fm.	San Joaquin Fm.	Etchegoin Fm.	Reef Ridge Fm.	Monterey Fm.
4029109250000	86-3	3 31S 26E	12,517	15	5,380	6,460	8,340	8,550
4029323490000	13-1	13 31S 26E	13,733			4,000	8,100	10,500
4029216330000	38-19	19 31S 26E	11,465		3,320	6,050	8,360	10,600
4029036870000	12-23	23 31S 26E	14,945		4,280	6,260	9,150	10,685
4029216370001	32-29	29 31S 26E	12,026	10	3,500	5,550	8,380	
4029293320000	61-31	31 31S 26E	12,995		3,220	5,740	7,860	10,030
4029196940001	18-36	36 31S 26E	12,232	12	4,710	6,530	10,350	11,130
4029323470000	1	6 31S 26E	10,250		3,790	4,700	7,690	8,650
4029733770000	22-9	9 31S 26E	10,400			5,700	8,810	9,250
4029854620000	1-25	25 31S 26E	14,014	32	5,250	7,290	9,900	11,610
4029216610000	87-28	28 31S 26E	11,796		4,110	6,050	9,270	
4029575740001	537-14R	14 30S 23E	13,500	25	910	3,120	5,170	7,900
4029685920000	562-20R	20 30S 23E	13,000	20	1,200	2,950	5,530	8,900
4029536860000	987-25R	25 30S 23E	18,761	24	800	3,990	5,210	5,800
4029719530000	514-30R	30 30S 23E	13,250		1,200	2,790	5,070	7,120
4029529320000	56X-10	10 30S 24E	13,528			4,670	5,560	10,300
4029374740000	55	15 30S 24E	11,315	12	1,200	4,170	5,035	10,000
4029452960000	521-26S	26 30S 24E	11,478	12	550	4,360	4,840	9,260
4029589160000	577-34S	34 30S 24E	11,950	18	650	3,310	4,560	6,220
4029726050000	1-13	13 30S 24E	11,300			5,735	6,770	9,800
4029321610000	87-4	4 30S 25E	13,957	2,010	3,230	3,940	7,320	9,000
4029185650000	1	12 30S 25E	14,224		2,350	3,840	7,055	8,330
4029205440000	KCL15X-24	24 30S 25E	15,739	7	2,982	3,750	6,870	7,677
4029010640000	KCL33-26	26 30S 25E	13,930		1,990	4,950	8,330	9,050
4029606500000	26-29	29 30S 25E	17,978			4,500	6,720	7,640
4029152930000	21-33	33 30S 25E	14,003	0		1,905	7,300	7,700
4029042400000	12	3 30S 26E	13,131		2,650	3,800	6,170	7,200
4029444210000	44X-6	6 30S 26E	13,140	2,320	3,070	3,790	7,180	8,170
4029043360000	1-V-13	13 30S 26E	14,073				6,390	6,850
4029043210000	2	14 30S 26E	14,051				6,310	71,110
999999999	85X-18	18 30s 26E	13,626	20	3,500	5,590	7,190	8,330
4029428390001	21A-36	21 30S 26E	10,463		3,500	4,350	6,380	7,310
4029043930001	34-25	25 30S 26E	10,656				6,940	7,320
4029002750100	53-30	30 30S 26E	14,000		2,250	3,680	6,400	7,370
4029000040000	64-34	34 30S 26E	16,322	13	2,800	4,350	7,330	7,850
4029321940000	77-5	5 30S 27E	12,222			4,920	5,450	9,000
4029322130000	1	9 30S 27E	13,142				5,820	11,930
4029723680000	1-14	14 30S 27E	13,376			5,670	6,680	9,970
4029321990000	2	15 30S 27E	13,690				6,045	6,890
4029738550000	34X-20	20 30S 27E	12,015				6,395	7,350
4029580170000	14	22 30S 27E	13,532				5,690	7,800
4029820620000	1	25 30S 27E	14,700				7,550	8,590
4029654870000	16-30	30 30S 27E	14,786		6,850	7,462	11,850	14,130
4029322040000	71-33	33 30S 27E	12,355			3,670	6,399	7,300
4029772840000	36-1	36 30S 27E	12,865				7,480	8,530
4029553270000	27X-26	26 12N 21W	16,548	20	6,190	10,840	13,120	14,520
4029564310000	77X	28 12N 21W	14,775	25	5,760	10,210	12,520	13,850
4029398410000	88.00	32 12N 21W	12,658					

API	Well #	Location	Driller TD (ft)	TOP OF UNIT (Measured depths in feet)				
				Tulare Fm.	San Joaquin Fm.	Etchegoin Fm.	Reef Ridge Fm.	Monterey Fm.
4029611210000	27X-35	35 12N 21W	14,952	26	5,710	10,415	12,650	13,880
4029591800000	84	32 12N 22W	14,678	25	3,400	8,167	10,590	12,200
4029595190000	83X	33 12N 22W	13,778	30	3,450	8,750	11,162	12,550
4029590900000	67X	34 12N 22W	13,816	30	3,890	8,700	11,180	11,970
4029841740000	1	36 12N 22W	13,185	25	4,225	9,042	11,659	12,361
4030026310000	1	35 12N 23W	12,898			6,930	7,740	10,000
4029114200000	86	36 12N 23W	11,026	12	2,175	5,360	8,910	108,000
4029327680001	22-15	15 11N 20W	16,421			4,280	5,580	6,625
4029109460001	65-24	24 11N 20W	12,344				4,400	5,940
4029823830000	145-26	26 11N 20W	13,093				3,220	3,550
4029209010000	2-337	27 11N 20W	12,514				1,802	
4029797220000	31X-32	32 11N 20W	11,150		3,320	5,442	8,082	8,330
4029760620000	12420	34 11N 20W	13,249				3,960	5,100
4029157890000	87-3	3 11N 21W	12,899		5,200	9,890	12,250	13,430
4029157930000	841-5	5 11N 21W	13,960	15	4,100	8,870	11,710	12,500
4029158200000	33-15	15 11N 21W	14,471		5,030	10,030	12,170	13,160
4029850230000	32X-20	20 11N 21W	14,325			10,590	13,110	13,588
4029863230000	41X-12	12 11N 21W	16,110	27	4,750	11,200	14,741	
4029137090100	16X-26	26 11N 22W	12,500		2,080	4,275	8,280	
4029352970000	27	10 11N 22W	12,446		3,980	8,400	10,050	11,050
4029375840000	1	23 11N 22W	12,400	14	4,600	7,200	11,000	
4029497230000	21	13 11N 22W	22,029	29	3,870	8,540	10,300	11,020
4029543310000	75X-12	12 11N 22W	12,200	20	3,690	8,600	10,820	11,115
4029544640000	65-4	4 11N 22W	16,300	15	3,378	8,700	9,955	10,980
4029835740000	57X-24	24 11N 22W	12,642	24	5,715	7,590	11,700	11,990
4029861610000	65X-6	6 11N 22W	11,600			7,392	9,750	10,300
4029094080000	34	32 11N 22W	10,017			807	1,030	3,002
4029642850000	88X-1K	1 11N 23W	10,057	18	1,570	6,440	8,420	8,840
4029472940000	1-28	28 11N 23W	12,523	20	1,050	3,440		
4029013000000	1	35 11N 23W	13,131	15	700	3,900	4,980	5,880
4029153890000	1	32 11N 24W	7,037			600		1,250
4029216300000	31	12 11N 24W	5,793			630	770	
4029379840000	27-3	3 11N 24W	5,082			140	600	